

INSTITUTO NACIONAL DE PESQUISAS DA AMAZÔNIA – INPA
UNIVERSIDADE DO ESTADO DO AMAZONAS - UEA
Programa Integrado de Pós-Graduação - Clima e Ambiente – PPG-CLIAMB

**Estudo da advecção horizontal de CO₂ em florestas na Amazônia e sua
influência no balanço de Carbono**

JULIO TÓTA

Manaus, Amazonas
Outubro 2009

INSTITUTO NACIONAL DE PESQUISAS DA AMAZÔNIA – INPA
UNIVERSIDADE DO ESTADO DO AMAZONAS - UEA
Programa Integrado de Pós-Graduação - Clima e Ambiente – PPG-CLIAMB

**Estudo da advecção horizontal de CO₂ em florestas na Amazônia e sua
influência no balanço de Carbono**

JULIO TÓTA

Orientador: Dra. MARIA ASSUNÇÃO FAUS DA SILVA DIAS

Co-Orientador: Dr. DAVID ROY FITZJARRALD

Tese de doutorado apresentada ao PPG-
CLIAMB como parte dos requisitos
para obtenção do título de Doutor em
Clima e Ambiente, área de
concentração: Geociências.

Manaus, Amazonas

Outubro 2009.

C586e Silva, Julio Tóta da

Estudo da advecção horizontal de CO₂ em florestas na Amazônia e sua influência no balanço de carbono / Julio Tóta da Silva. -- Manaus : [s.n.], 2009.

xviii, 93 f. : il. (algumas color.)

Tese (doutorado em Clima e Ambiente)--INPA/UEA, Manaus, 2009.

Orientadora: Maria Assunção Faus da Silva Dias

Co-orientador: David Roy Fitzjarrald

Área de concentração: Interações Clima-Biosfera na Amazônia

1.Advecção-Carbono 2.Florestas tropicais-Amazônia 3.Vórtices turbulentos I.Título

CDD 19^a ed. 551.5112

Sinopse:

Este estudo apresenta observações da dinâmica do escoamento do vento dentro e acima em área de Floresta Tropical na Amazônia, verificando sua relação com o transporte horizontal de CO₂ sobre terrenos de topografia complexa e avaliando seu impacto no balanço de carbono com o uso do sistema de correlações de vórtices turbulentos (Eddy Correlation System).

Palavras-chaves: Advecção Horizontal de CO₂, Floresta Tropical, Amazônia, Escoamento de drenagem; Sistema de Correlações de Vórtices Turbulentos, CO₂.

Dedico

*Aos meus pais Antonio Tota e Severina
Soares, e aos meus filhos Luny Tota e Luan Tota*

Agradecimentos

A Deus,

Ao Instituto Nacional de Pesquisas da Amazônia (INPA), pela oportunidade de formação,

À Fundação de Amparo a Pesquisa do Estado do Amazonas (FAPEAM) pela bolsa de estudos,

Agradeço ao Conselho Nacional de Desenvolvimento Científico e Tecnológico – CNPq,

Eu sou especialmente grato aos meus orientadores Dra. Maria Assunção e Dr. David Fitzjarrald, pela paciência, orientação e apoio constante e pela amizade,

Agradeço aos membros da banca pelas sugestões e revisão do texto da tese,

Expresso minha gratidão ao Dr. Manzi, Coordenador do Programa de Pós-Graduação em Clima e Ambiente (CLIAMB-INPA/UEA), pelo constante encorajamento, a atenção e pela amizade desses muito anos,

Agradeço a todos os amigos que me ajudaram nesse caminho: Hermes, Amaury, Juliana, Julio, Galúcio, Madruga, Alessandro, Celso, Betânia, Veber, e muitos... Todos os funcionários do LBA Manaus, eu sou grato por todo o apoio logístico,

Especial obrigado para Claudia Vitel e Edwin Keiser pela amizade e apoio,

Aos professores do Programa CLIAMB-INPA/UEA e aos colegas de classe,

RESUMO

Fluxos horizontais e verticais de CO₂ foram feitos na floresta tropical na Amazônia dentro da Reserva de Floresta Nacional do Tapajós (FLONA-Tapajós - 54°58'W, 2°51'S). Duas campanhas de medidas observacionais foram conduzidas em 2003 e 2004 para descrever o escoamento abaixo do dossel, determinar sua relação com o vento acima da floresta, e estimar como este escoamento transporta CO₂ horizontalmente. Atualmente já está reconhecido que o transporte horizontal de CO₂ respirado abaixo da floresta não está representado pelo balanço obtido somente em um ponto de medida nas torres de fluxos (Eddy Covariance - EC), com erros mais significativos sob condições de noites calmas. Neste trabalho testamos a hipótese de que o transporte horizontal médio, anteriormente não medido em florestas tropicais, possa representar a quantidade de CO₂ respirado destas condições. Foi instalada uma rede de sensores de vento e CO₂ abaixo da vegetação. Um significativo transporte horizontal de CO₂ foi observado nos primeiros 10 metros da floresta. Os resultados indicaram que a advecção de CO₂, para todas as noites calmas estudadas, representou 73 e 71% do déficit noturno, definido pela diferença entre a respiração total do ecossistema (medida ecológica) e o fluxo medido pelo sistema EC na torre de fluxo, durante as estações seca e chuvosa, respectivamente. Foi também encontrado que a advecção horizontal de CO₂ noturna é igualmente importante, tanto para condições de baixos níveis de turbulência como para aquelas com altos valores de velocidade de fricção (nível de turbulência), sendo estes limiares comumente usados para correções dos fluxos noturnos (correção por u_*). Sobre uma área de terreno complexa coberta por floresta tropical densa (Reserva Biológica do Cuieiras – ZF2 - 02°36'17.1"S, 60°12'24.5"W) foram medidos gradientes horizontais e verticais de temperatura do ar, concentrações de CO₂ e o campo de vento durante as estações seca e chuvosa de 2006. Foi testada a hipótese de que escoamento de drenagem horizontal sobre a área de estudo é significativa e pode afetar a interpretação das altas taxas de absorção de carbono reportadas por trabalhos anteriores. Um experimento de campo similar ao desenvolvido por Tóta et al. (2008) foi usado, incluindo uma rede de sensores de vento, temperatura do ar e concentração de CO₂, acima e abaixo da floresta. Foi observado um padrão de escoamento abaixo da floresta, persistente e sistemático, sobre uma área de encosta de moderada inclinação (~12%), subindo durante a noite (associada com flutuabilidade positiva) e descendo durante o dia (flutuabilidade negativa). Acima da floresta (38m) sobre a mesma área de encosta foi também observado um movimento vertical descendente indicando convergência vertical e correspondente divergência horizontal em direção ao centro do vale próximo a torre de

medida. Foi observado que as micro-circulações acima da floresta foram dirigidas pelo balanço entre as forças gradiente de pressão e de flutuabilidade (buoyancy), e abaixo da floresta também foram dirigidas pelo mesmo mecanismo físico. Os resultados também indicaram que os gradientes horizontais e verticais de CO₂ foram modulados pelas micro-circulações acima e abaixo da vegetação, sugerindo que as estimativas da advecção usando a estratégia experimental anterior não são apropriadas devido a natureza tri-dimensional do transporte horizontal e vertical do local.

SUMMARY

Horizontal and vertical CO₂ fluxes and gradients were obtained in an Amazon tropical rain forest, the Tapajós National Forest Reserve (FLONA-Tapajós - 54°58'W, 2°51'S). Two observational campaigns in 2003 and 2004 were conducted to describe subcanopy flows, clarify their relationship to winds above the forest, and estimate how they may transport CO₂ horizontally. It is now recognized that subcanopy transport of respired CO₂ is missed by budgets that rely only on single point Eddy Covariance measurements, with the error being most important under nocturnal calm conditions. We tested the hypothesis that horizontal mean transport, not previously measured in tropical forests, may account for the missing CO₂ in such conditions. A subcanopy network of wind and CO₂ sensors was installed. Significant horizontal transport of CO₂ was observed in the lowest 10m of the canopy. Results indicate that CO₂ advection accounted for 73% and 71%, respectively of the carbon budget deficit (difference between total ecosystem respiration and respective eddy flux tower measured) for all calm nights evaluated during dry and wet periods. We found that horizontal advection was significant to the canopy CO₂ budget even for conditions with the above-canopy friction velocity higher than commonly used thresholds (u_* correction). On the moderate complex terrain cover by dense tropical Amazon rainforest (Reserva Biológica do Cuieiras – ZF2 - 02°36'17.1"S, 60°12'24.5"W) subcanopy horizontal and vertical gradients of the air temperature, CO₂ concentration and wind field were measured for dry and wet periods in 2006. We tested the hypothesis that horizontal drainage flow over this study area is significant and it can affect the interpretation of the high carbon uptake reported by previous works. A similar experimental design to the one by *Tota et al.* (2008) was used with subcanopy network of wind, air temperature and CO₂ sensors above and below the forest canopy. It was observed a persistent and systematic subcanopy nighttime upsloping (positive buoyancy) and daytime downsloping (negative buoyancy) flow pattern on the moderate slope (~12%) area. Above canopy (38 m) on the slope area was also observed a downward motion indicating vertical convergence and correspondent horizontal divergence into the valley area direction. It was observed that the micro-circulations above canopy were driven mainly by the balancing pressure and buoyancy forces and that in subcanopy was driven similar physical mechanisms. The results also indicated that the horizontal and vertical scalar gradients (e.g. CO₂) were modulated by these micro-circulations above and below canopy, suggesting that advection estimates using the previous experimental approach is not appropriate due to the tri-dimensional nature of the vertical and horizontal transport locally.

LISTA DE FIGURAS

Capítulo I: Amazon rain Forest subcanopy flow and the carbon budget: Santarém LBA-ECO Site.

- Figura 1.** Site Location in the vegetation cover image and high resolution (30m grid space) tower-base local topography as determined by the Shuttle Radar Topography Mission (SRTM). The arrows shows the modal wind direction at 57.8 m (red, from East) and in the subcanopy (magenta, from southeast)..... 22
- Figure 2.** Main tower and Draino deployed instruments systems.....23
- Figure 3.** The autocorrelation coefficient for total wind speed (left panel) and CO₂ concentration (center panel) as a function of distance between sampling points 1.8m above ground in the subcanopy. (3-minute averages data from “Draino” Phase 1 (DOY 198-238/2003). “C” represents the calibration period. The right panel shows the temporal autocorrelation, the solid line represents the median, and the thinner lines the upper and lower quartiles. Mean wind speed in the subcanopy was 0.13 m/s.27
- Figure 4.** Typical nighttime normalized median profiles of CO₂, wind speed and their product (uc) horizontal transport (left panel); and the diurnal cycle of the shape factor for horizontal advection (right panel).30
- Figure 5.** Night time composite of averaged subcanopy CO₂ concentration field and wind vectors for Phase 1 and Phase 2 campaigns. The units are in ppm and ms⁻¹, respectively. (Largest arrow is 0.15 m s⁻¹).....32
- Figure 6.** Vertical profiles of concentration of CO₂, wind speed, temperature, and water vapor, for both Phases (dry and wet)33
- Figure 7.** Frequency distribution histogram of friction velocity (u*) at 57.8 m, for Phase 1 and Phase 2 measurements, separate day and night periods.34
- Figure 8.** Nighttime distribution of the wind rose and its magnitude (m s⁻¹) for the Draino sonic anemometer network and at top of main tower (57.8 m), including its localization see Figure 2).37
- Figure 9.** Diurnal cycle of buoyancy term forcing fractions relative to stress divergence term for Phase 1 (top panel) and Phase 2 (middle panel) observations, and (bottom panel) the buoyancy forcing term vs. subcanopy wind direction.38

Figure 10a. Hourly-averaged summary of results for the Phase 1 and all the terms except eddy flux are average values for 0 to 57.8 m control volume. Top panel: vertical eddy flux at 57.8 m; 2nd panel: storage; 3th panel: east-west advection; and 4th panel: south-north advection, terms.	39
Figure 10b. Hourly-averaged summary of results for the Phase 2 and all the terms except eddy flux are average values for 0 to 57.8 m control volume. Top panel: vertical eddy flux at 57.8 m; 2nd panel: storage; 3rd panel: vertical advection; 4th panel: east-west advection; and 5th panel: and south-north advection, terms.	40
Figure 11a. Top panel: Hourly-averaged vertical eddy flux at 57.8 m; 2nd panel: storage term; 3rd panel: east-west advection term; and 4th panel: and south-north advection, terms. Note the change in vertical scale between the phases.	41
Figure 11b. Top panel: Hourly-averaged vertical eddy flux at 57.8 m; 2nd panel: storage term; 3rd panel: vertical advection term; 4th panel: east-west advection term; and 5th panel: and south-north advection terms. Note the change in vertical scale between the phases....	42
Figure 12a. Mean nocturnal variation of the NEE (Eddy covariance flux + storage), ecosystem respiration, horizontal advection and NEE plus advection, for Phase 1 (Dry period).	43
Figure 12b. Same Figure 12a, for Phase 2 (Wet period).	44
Figure 13. Mean nocturnal variation of the advection term as a function of the friction velocity rank, for Phase 1 (left panel) and Phase 2 (right panel) datasets. Solid line with dots indicates binned average values (0.1 intervals)). Error-bar also is plot with standard deviation, respectively.	45

Capítulo II: Amazon rain Forest subcanopy flow and the carbon budget: Manaus LBA Site - a complex terrain condition.

Figure 1. Detailed measurements towers's view in the ZF-2 Açu catchment (East-West valley orientation) from SRTM-DEM datasets. Large view in the above panel and below panel the points of measurements (B34 – Valley, K34 – Plateau, and subcanopy Draino system measurements over slopes in south and north faces (red square points).....	51
Figure 2. (a) Açu Cachment with level terrain cotes and vegetation cover from IKONOS's image and (b) vegetation structure measured from Lidar sensor over yellow transect (a). From (a) the blue color is valley and vegetation transition to plateau areas (red colors)....	52

Figure 3. Draino measurement system used in Manaus LBA (South Face, see also Figure 4).....	54
Figure 4. Draino measurement system (South and North Slope face) implemented at Manaus LBA Site, including topographic view and instrumentation deployed.....	55
Figure 5. 10 days time series of the CO ₂ concentration, air temperature (DRAINO System) and total precipitation (plateau tower).....	57
Figure 6. Boxplot of the virtual potential temperature vertical profile for dry (a, b) and wet periods (c,d) of the 2006 during night (b,d) and daytime (a,c), on the plateau K34 tower..	59
Figure 7. Daily course of the vertical deviation of the virtual potential temperature for dry (a) and wet (b) periods of the 2006, on the plateau K34 tower.....	60
Figure 8. Boxplot of the virtual potential temperature vertical profile for dry (a, b) and wet periods (c, d) of the 2006 during night (b, d) and daytime (a, c), on the slope area DRAINO System tower (south face, see Figure 2).....	61
Figure 9. Daily course of the vertical deviation of the virtual potential temperature for dry (a) and wet (b) periods of the 2006, and virtual potential temperature vertical gradient (c), on the slope area DRAINO System tower.....	62
Figure 10. Frequency distribution of the wind speed and direction. For dry (a, b) and wet (c, d) periods from 2006 during day (a, c) and nighttime (b, d), on the plateau K34 tower.....	64
Figure 11. Frequency distribution of the wind speed and direction above canopy (38 m above ground level – a.g.l). For dry (a, b) and wet (c, d) periods from 2006 during day (a, c) and nighttime (b, d), on the slope area at DRAINO system tower.....	65
Figure 12. Frequency distribution of the wind speed and direction in the subcanopy array (2 m above ground level – a.g.l) on the microbasin south face slope area at DRAINO horizontal array system (see Figure 4). For dry (a-f) and wet (g-l) periods from 2006, during day (a, b, c, g, h, i) and nighttime (d, e, f, j, k, l).....	67
Figure 13. Frequency distribution of the subcanopy wind direction (a) upsloping (from north quadrant) and (b) downsloping (from south quadrant) on the south face slope area at DRAINO horizontal array system (see Figure 4).....	69
Figure 14. Mean vertical velocity raw and correct vertical velocity (a) for DRAINO system slope tower (38 m), and hourly mean vertical velocity (b) for: plateau K34 tower (55 m), DRAINO system slope tower (above canopy - 38 m and subcanopy - 3 m) and for valley B34 (43 m) towers (see Figure 4, for details).....	70
Figure 15. Schematic local circulations in the site studied, valley and slopes flow (a), 2D view from suggested below and above canopy airflow (b).....	72

- Figure 16.** Example at midnight (local time) of the horizontal CO₂ concentration over the DRAINNO System south face domain including an interpolated horizontal wind field (10 m grid), note the geographic orientation and the red arrow indicating slope inclination (see Figure 4).....74
- Figure 17.** Hourly average of the subcanopy (2 m) CO₂ concentration and horizontal wind speed over DRAINNO System south face area during dry period of the 2006, note the geographic orientation and the red arrow indicating slope inclination (see Figure 4). The axis represents distances from center of the main tower.....75
- Figure 18.** Hourly average of the subcanopy (2 m) CO₂ concentration on the DRAINNO System north face area during dry period of the 2006, note the geographic orientation (see Figure 4). The axis represents distances from center of the main tower.....76

SUMÁRIO

INTRODUÇÃO GERAL.....	14
OBJETIVO GERAL.....	16
OBJETIVOS ESPECÍFICOS.....	16
Capítulo I: Amazon rain forest subcanopy flow and the carbon budget: Santarém LBA-ECO	18
Abstract	18
1. Introduction	19
2. Material and Methods	21
2.1 Site description	21
2.2. Instrumentation and observation	23
2.3. Preinstallation intercomparison	26
2.4. CO ₂ conservation equations	28
2.5. Vertical integration of the horizontal advection terms	30
3 – Results and Discussion	32
3.1. CO ₂ concentration field	32
3.2. Subcanopy horizontal wind field	36
3.3. Subcanopy flow forcing terms	37
3.4. Estimates of Advection Terms	39
3.5. CO ₂ budget	43
3.6. Correlation between advection components and friction velocity	44
4. Summary and Conclusions	45
Capítulo II: Amazon rain Forest subcanopy flow and the carbon budget: Manaus LBA Site - a complex terrain condition	48
Abstract	48
1. Introduction	49
2. Material and Methods	50
2.1 Site description	50
2.2. Measurements and instrumentation	53

3 – Results and Discussion	57
3.1. Air Temperature field	58
3.1.1 - Plateau K34 tower	58
3.1.2 – DRAINNO System Slope tower	60
3.2. Wind field	63
3.2.1 – Horizontal wind regime - above canopy.....	63
3.2.1.1 - Plateau K34 tower	63
3.2.1.2 - DRAINNO System slope tower	64
3.2.2 – Horizontal wind regime – Subcanopy array measurements (2 m a.g.l)	65
3.2.3 – Mean Vertical wind velocity – subcanopy and above canopy	69
3.3. Phenomenology of the local circulations: Summary	72
3.4. CO ₂ concentration and subcanopy horizontal wind field	73
4. Summary and Conclusions	77
CONCLUSÃO GERAL.....	79
REFERÊNCIAS.....	82

INTRODUÇÃO GERAL

Nas últimas décadas há um crescente interesse da comunidade científica em quantificar as trocas líquidas de dióxido de carbono (CO_2) entre ecossistemas florestais e a atmosfera, devido ao nível de incerteza das estimativas das fontes e sumidouros desses ecossistemas no balanço global de carbono. Enquanto as estimativas do crescente nível de aumento de CO_2 atmosférico e os sumidouros de CO_2 pelos oceanos são bem conhecidas, as fontes e sumidouros da biosfera ainda não são estimados precisamente (IPCC 2007). Reduzir as incertezas das fontes e sumidouros de dióxido de carbono da biosfera tem sido um grande desafio da comunidade científica atualmente visando melhor entender o balanço global de carbono e o papel dos biomas terrestres no assim chamado “aquecimento global”.

Os biomas florestais exercem um papel importante no balanço global de carbono, pois representam 80% de biomassa aérea e 40% de biomassa de raízes e serrapilheira do carbono orgânico global (Dixon et al., 1994). Dentre estes ecossistemas, as florestas tropicais da Amazônia são uma importante componente para o balanço global de carbono, em função da sua grande quantidade de biomassa armazenada e de seu rápido ciclo de carbono através dos processos de fotossíntese e respiração. As florestas da Amazônia representam 10% da produtividade primária terrestre e do carbono armazenado nos ecossistemas terrestres (Melillo et al., 1993; Malhi et al., 1998). Portanto, para melhor quantificar o balanço global de carbono é preciso também determinar o balanço regional de carbono na Amazônia e sua variabilidade em resposta as mudanças do meio ambiente. Para isso, torna-se crítico entender os processos de respiração e fotossíntese do ecossistema Amazônico detalhadamente.

Atualmente não há um consenso da comunidade científica se as florestas tropicais na Amazônia atuam como fontes ou sumidouros de CO_2 atmosférico. Estimativas com base em medidas biométricas, sugerem tanto um papel de sumidouro (Phillips et al., 1998; Baker et al., 2004), como uma fonte de CO_2 atmosférico (Rice et al., 1998; Miller et al., 2004). Por outro lado, estimativas com base em medidas pelo método das covariâncias de vórtices turbulentos (EC – “Eddy covariance System”), sugerem que o ecossistema de floresta tropical na Amazônia atua como sumidouro (Grace et al., 1995; Malhi et al., 1998; Araújo et al., 2002), uma pequena fonte (Saleska et al., 2003; Huttyra et al., 2007), ou em equilíbrio (Miller et al., 2004), com relação às trocas líquidas de CO_2 atmosférico.

Portanto, existe uma urgente necessidade em melhor entender e quantificar as incertezas dessas estimativas em ecossistemas terrestres, em especial na Amazônia.

As estimativas realizadas por EC na escala espacial das torres micrometeorológicas, são uma importante ferramenta para quantificar as trocas líquidas entre a superfície e a atmosfera e amplamente utilizada desde seu desenvolvimento (Montgomery, 1948; Swinbank, 1951) para estimativas das trocas de energia (Antonia et al., 1979; Fitzjarrald et al., 1988; Bergstrom and Hogstrom, 1989; Gao et al., 1989; Shuttleworth, 1989) e gases traços, como CO₂ (Fan et al., 1990; Lee et al., 1992; Wofsy et al., 1993; Grace et al., 1995; Black et al., 1996; Moncrieff et al., 1997; Malhi et al., 1998; Baldocchi et al., 2001; Araújo et al., 2002). A metodologia de EC tem a vantagem de obter medidas diretas e de longo prazo dos fluxos de CO₂ na interface floresta-atmosfera (Wofsy et al., 1993; Goulden et al., 1996; Urbanski et al., 2007).

Entretanto, teoricamente este método assume que as áreas representativas das medidas sejam horizontalmente homogêneas e planas para uma melhor estimativa dos fluxos turbulentos obtidos pelas torres. Dessa forma, considera que a mistura turbulenta atmosférica seja suficientemente efetiva para eliminar o efeito da variabilidade da cobertura da superfície em pequena escala (tipo de vegetação e terreno) e represente o fluxo turbulento médio da área obtido nas torres de fluxos.

Em termos de balanço de energia ou de gases, isto significa que os termos de transportes horizontais (advecção) são desprezados ou não significativos, predominando apenas os fluxos verticais turbulentos. Isto tem um efeito significativo nas trocas líquidas entre o ecossistema e a atmosfera (NEE – “Net Ecosystem Exchange”), a qual é obtida, neste caso, somente pela soma dos fluxos verticais turbulentos e o termo de armazenamento (Storage) abaixo do nível da medida ($NEE = \text{Eddy Flux} + \text{Storage}$). O termo de armazenamento, por exemplo, na Amazônia, tem sido obtido raramente de maneira contínua, dada as dificuldades específicas de cada sítio e das condições ambientais adversas, gerando uma barreira para as estimativas de NEE (Iwata et al., 2005).

Sob certas condições de baixo nível de turbulência atmosférica (geralmente nos períodos noturnos) e certo grau de complexidade topográfica, circulações secundárias e escoamento horizontal sobre as encostas do terreno, o chamado escoamento de drenagem (“Drainage Flow”), podem se desenvolver (Yoshino et al., 1984). Isto tem sido evidenciado por vários estudos em diversas localidades, os quais indicam a importância da advecção de CO₂ no balanço de carbono (Aubinet et al., 2003; Staebler and Fitzjarrald, 2004, 2005; Marcolla et al., 2005; Feigenwinter et al., 2008; Leuning et al., 2008). Porém, os estudos de

advecção de CO₂ foram realizados sobre regiões montanhosas de latitude média e não em regiões de florestas tropicais, passando a ser uma motivação e um desafio, investigar a existência e quantificar a importância da advecção de CO₂ no balanço de carbono das áreas de floresta tropicais na Amazônia.

Com o objetivo de quantificar e melhor entender as fontes e sumidouros de CO₂ na região de floresta tropical na Amazônia, o Projeto de Grande Escala da Biosfera-Atmosfera na Amazônia (LBA - “Large Scale Biosphere-Atmosphere experiment in Amazonia”) estabeleceu uma rede de torres micrometeorológicas com o sistema EC em vários pontos na região (Keller et al., 2004).

Esta tese visa investigar os processos de transporte não turbulentos, os quais são os termos advectivos componentes da equação de balanço de carbono, e os mecanismos físicos que os dirigem, nos sítios experimentais do Projeto LBA de Santarém (PA) e de Manaus (AM). Para isso, foi concebido um sistema de medida direta e detalhada das principais variáveis (velocidade do vento, temperatura do ar e concentração de CO₂) usadas para caracterizar a dinâmica do escoamento acima e abaixo da floresta, e calcular os termos advectivos de transporte de CO₂ sobre as áreas representativas das torres micrometeorológicas do projeto LBA.

OBJETIVO GERAL

Esta tese tem como objetivo geral investigar e quantificar através de medidas observacionais os mecanismos físicos que dirigem os termos não turbulentos das equações de balanço de carbono associados com o transporte lateral de CO₂ em dois sítios de floresta tropical do projeto LBA na Amazônia.

OBJETIVOS ESPECÍFICOS

- 1) Implementar um sistema de medidas observacional para investigar a dinâmica do escoamento acima e abaixo da floresta tropical na Amazônia sobre terrenos complexos, capaz de medir baixos limiares de velocidade do vento e gradientes horizontais de CO₂ abaixo da copa da floresta;

- 2) Determinar e quantificar os gradientes horizontais e verticais de concentrações de CO₂ importantes para os transportes horizontais de CO₂, (advecção horizontal – Capítulo I – Sítio do LBA em Santarém - PA);
- 3) Avaliar e/ou determinar a existência do escoamento horizontal abaixo da copa da floresta, bem como, sua persistência e sistemática em produzir transporte horizontal de CO₂ para fora da área de representatividade do sistema EC das torres micrometeorológicas do projeto LBA e determinar sua validade;
- 4) Determinar os mecanismos físicos da dinâmica do escoamento responsáveis pela advecção horizontal de CO₂;
- 5) Quantificar os termos de transportes horizontais e/ou advecção horizontal de CO₂, que contribuem para o balanço de carbono na escala das torres micrometeorológicas do LBA;

**Capítulo I - Amazon rain forest subcanopy flow and the carbon budget:
Part I – Santarém LBA-ECO ¹**

Abstract

Horizontal and vertical CO₂ fluxes and gradients were obtained in an Amazon tropical rain forest, the Tapajós National Forest Reserve (FLONA-Tapajós - 54°58'W, 2°51'S). Two observational campaigns in 2003 and 2004 were conducted to describe subcanopy flows, clarify their relationship to winds above the forest, and estimate how they may transport CO₂ horizontally. It is now recognized that subcanopy transport of respired CO₂ is missed by budgets that rely only on single point Eddy Covariance measurements, with the error being most important under nocturnal calm conditions. We tested the hypothesis that horizontal mean transport, not previously measured in tropical forests, may account for the missing CO₂ in such conditions. A subcanopy network of wind and CO₂ sensors was installed. Significant horizontal transport of CO₂ was observed in the lowest 10 m of the canopy. Results indicate that CO₂ advection accounted for 73% and 71%, respectively of the carbon budget *deficits* for all calm nights evaluated during dry and wet periods. We found that horizontal advection was significant and important to the canopy CO₂ budget, during environmental conditions with lower above-canopy friction velocity values and also during higher values commonly used thresholds to the u* corrections approach.

Key words: Amazon Rainforest; Advection, Drainage Flow, Eddy Covariance, Subcanopy.

¹ Tóta, J., Fitzjarrald, D.R., Staebler, R.M., Sakai, R.K., Moraes, O.M.M., Acevedo, O.C., Wofsy, S.C., Manzi, A.O., 2008. Amazon rain forest subcanopy flow and the carbon budget: Part I – Santarém LBA-ECO Site. *Journal of Geophysical Research – Biogeosciences*, 113, 1-15.

1. Introduction

In the last decade tower-based eddy-covariance (EC) observations have been established worldwide to monitor net ecosystem exchange (NEE) of carbon dioxide [Goulden *et al.*, 1996; Black *et al.*, 1996; Baldocchi *et al.*, 2001]. This micrometeorological method is considered the most accurate when applied at nearly flat sites that have long homogeneous upwind fetches. Its application has spawned global scale flux-measuring networks [Baldocchi *et al.*, 1988; Aubinet *et al.*, 2000] whose justification has been to estimate long-term carbon exchange. Two related issues complicate this ambition. First, proper estimates of nocturnal respiratory fluxes are essential, but weak turbulent mixing at night is common. This issue of underreporting of nocturnal CO₂ fluxes has been addressed using the approach advocated by Goulden *et al.* [1996], formalized by the FLUXNET committee [Baldocchi *et al.*, 2001]. Data on very calm nights (often an appreciable fraction of all nights) is simply discarded and replaced with the result of an ecosystem respiration rate found on windy nights that are otherwise similar [Miller *et al.*, 2004; Gu *et al.*, 2005]. A second issue is that many flux-observing sites lie in complex terrain [Lee, 1998; Paw U *et al.*, 2000; Aubinet *et al.*, 2003; Feigenwinter *et al.*, 2004; Staebler and Fitzjarrald, 2004, 2005]. On the very calm nights for which flux underestimates occur, subcanopy drainage flows are most common [Yoshino *et al.*, 1984; Sun *et al.*, 2007]. Whether or not subcanopy drainage flows also advect sufficient CO₂ laterally out of the budget “box” to account for the ‘missing flux’ on calm nights is site specific, and must be determined observationally [Lee, 1998; Feigenwinter *et al.*, 2004; Staebler and Fitzjarrald, 2004; Aubinet *et al.*, 2005]. Previous studies show that, under light wind and very stable conditions over the canopy, the importance of advection on the carbon balance can be as large as, or even larger than, the magnitude of NEE, observed by the EC approach when there are drainage flows [Staebler, 2003; Staebler and Fitzjarrald, 2004,

2005; *Sun et al.*, 2007]. To assess the importance of subcanopy flows one must present a plausible physical mechanism to account for this underestimation as past studies asserted [*Kruijt et al.*, 2004; *Araújo et al.*, 2002]. Even on gentle slopes, it is risky to assume that there is no lateral motion or divergence that can advect CO₂ (e.g., *Acevedo and Fitzjarrald*, 2003) and applying the ideal site criteria to more typical situations is questionable [*Baldocchi et al.*, 2000; *Staebler and Fitzjarrald*, 2004, 2005].

Most studies of subcanopy advection to date have been done at midlatitude sites. We are not aware of similar studies in the tropical rain forest. The forests in the Amazon region account for 10% of the world's terrestrial primary productivity and about the same fraction of carbon stored in land ecosystems [*Malhi et al.*, 1998]. In the last decade reports have suggested that this region has such a positive sink of CO₂, which, when scaled for the entire Amazon region, could account for a significant fraction of the carbon budget, the so called residual terrestrials sink (IPCC, 2007). Since results from the Large Scale Biosphere-Atmosphere experiment in Amazonia (LBA, *Keller et al.*, 2004) will likely be used to represent the Amazon in its entirety in global change models, it is important to identify systematic observation problems. In this paper we describe a detailed subcanopy CO₂ and wind system sensors deployed for the first time in the Amazon tropical rainforest combined with EC tower flux and respiration measurements and analyze the results with the aim to better understand the local carbon budget. Formally, we test the hypotheses that EC measurements underestimate the CO₂ flux on calm nights because of lateral air flow out of the control volume at the km67 Santarém LBA site. We seek to demonstrate that observed subcanopy horizontal CO₂ gradients and wind transport processes yield significant mean net transport of CO₂ into or out of the control volume. Following *Staebler and Fitzjarrald* [2004, 2005], we examine the importance of subcanopy advection in the following steps:

(1) We must show that systematic subcanopy flows exist and are measurable; and

(2) Observed subcanopy flows must be related to a physical driving mechanism (e.g. drainage forcing) that ensures that they are sufficiently systematic so that long-term budgets are affected.

2. Material and Methods

2.1. Site description

The study site (54° 58'W, 2° 51'S) is part of the ecological component of the Large Scale Biosphere-Atmosphere experiment in Amazonia (LBA-ECO), which aims to achieve better understanding of the regional carbon balance. It is located in the Tapajós National Forest reserve (FLONA Tapajós), near km 67 of the Santarém-Cuiabá highway (BR-163). The average temperature, humidity, and rainfall are 25.8°C, 85%, and about 1800 mm per year, respectively [Parotta *et al.*, 1995]. This area contains predominantly nutrient-poor clay oxisols with some sandy utisols [Silver *et al.*, 2000], each of which has low organic content and cation exchange capacity.

Vegetation consists of occasional 55 m height emergent trees with a closed canopy at 40m and below [Parker *et al.*, 2004]. Trees include *Manilkara huberi* (Ducke) Chev., *Hymenaea courbaril* L., *Betholletia excelsa* Humb. and Bonpl., and *Tachigalia spp* species, and epiphytes. There is overall an uneven age distribution, but the forest can be considered to be primary or old growth [Clark, 1996; Goulden *et al.*, 2004].

Local topographic features include a steep nearby river escarpment sloping to the Tapajós River to the west, but with a weak eastward-facing slope into the basin of the Curua-Una watershed. Except near the escarpment, drainage flows would be expected to move opposing the easterly prevailing wind field (red arrow in the Figure 1).

Several studies have demonstrated a significant seasonal variations in solar radiation, net radiation, air temperature, and vapor pressure deficit, all of which increase substantially with the seasonal decline in precipitation, while surface litter and soil moistures also decline [da Rocha *et al.*, 2004].

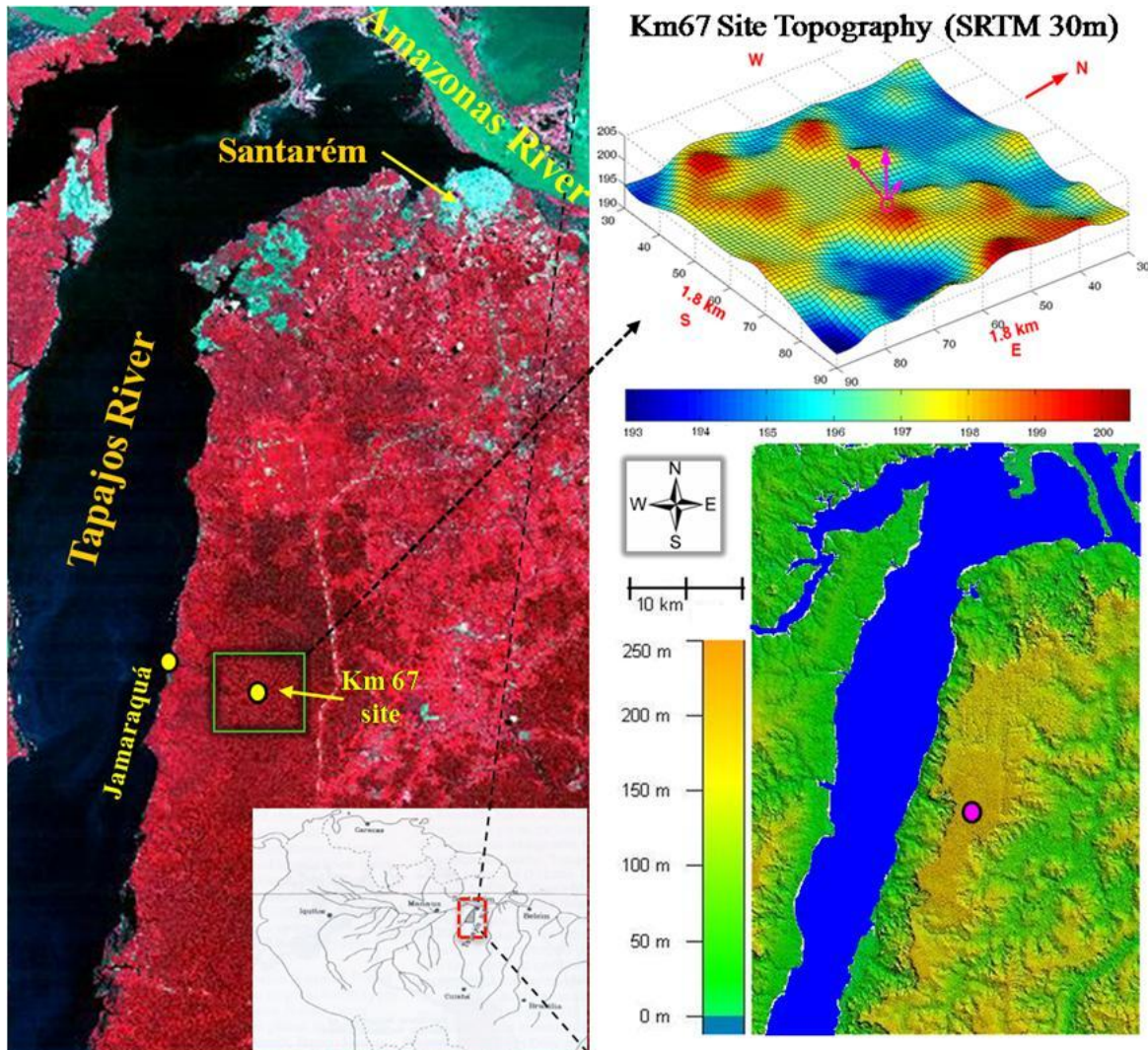


Figure 1. Site Location in the vegetation cover image and high resolution (30m grid space) tower-base local topography as determined by the Shuttle Radar Topography Mission (SRTM). The arrows shows the modal wind direction at 57.8 m (red, from East) and in the subcanopy (magenta, from southeast).

2.2. Instrumentation and observation

The field measurements at the old growth forest site at km67 in the LBA study area included several meteorological and EC measurements from 2001 to 2006, focusing on the dynamics of primary forest ecosystems. Several LBA groups have made observations of meteorological quantities, such as EC fluxes of H_2O , CO_2 , temperature, and wind fields. We share datasets obtained by the LBA Project groups CD03 and CD10 (CD – Carbon Dynamics).

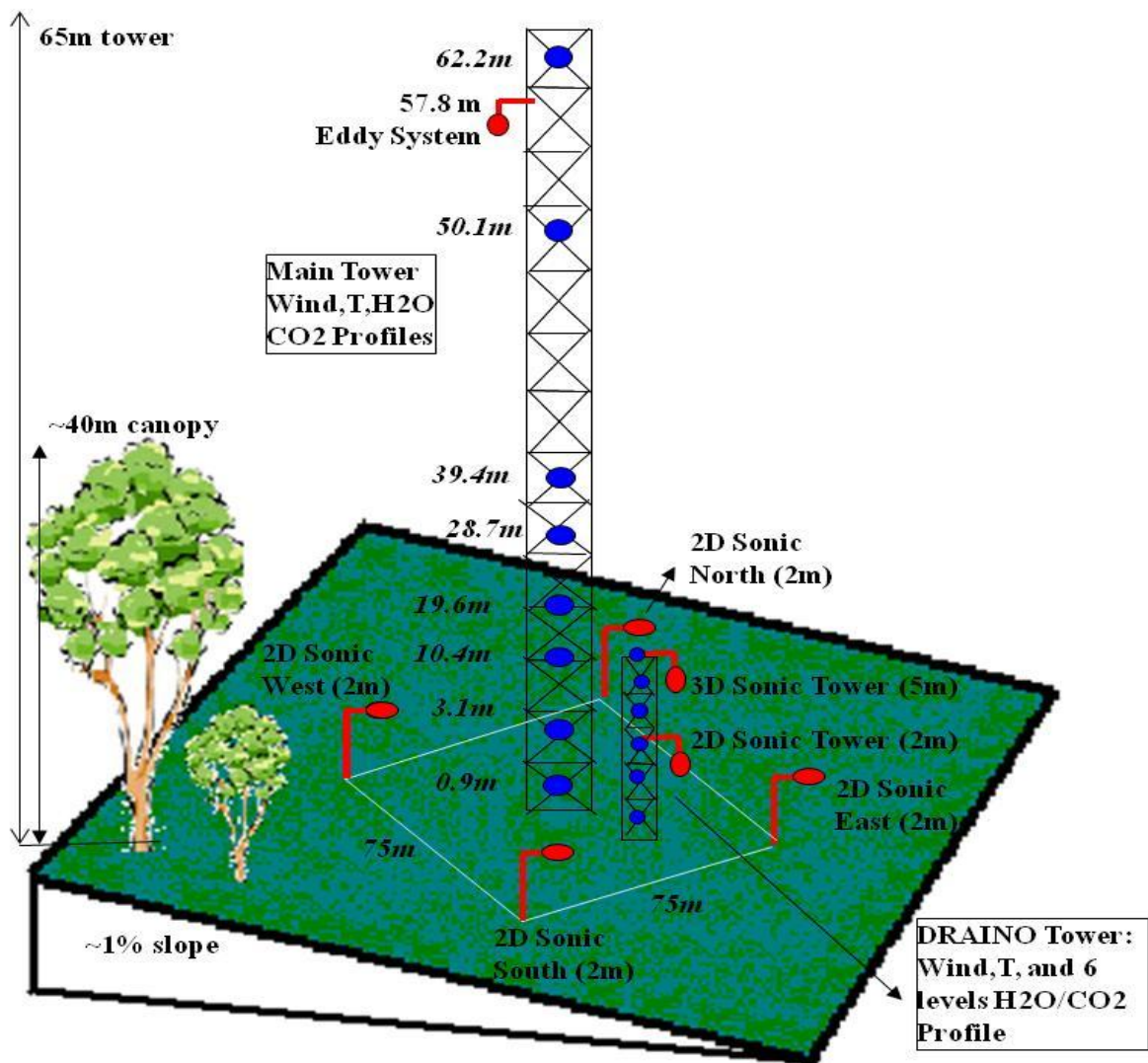


Figure 2. Main tower and Draino deployed instruments systems.

The CD10 tower systems include EC and meteorological wind, CO₂, temperature and water vapor profiles collected between 2001 and 2006 (Table 1 and Figure 2). The instrumentation descriptions and quality control procedures for the basic datasets obtained at the main km67 tower site are given in *Saleska et al.* [2003] or at the online web page <http://www-as.harvard.edu/data/lbadata.html>. A weather station was deployed in Jamaraguá at the base of the Tapajós escarpment to help in identifying topographical effects. A high resolution STRM map was made, based on a 90m grid, interpolated to 30 meters, to describe the gentle topography around the tower site (Figure 1).

Table 1. LBA – Old Growth (KM67) Site Sensors

Level (m)	Parameter	Instrument
64.1,52,38.2,30.7 57.8	Wind speed u' v' w' T', CO ₂ , H ₂ O	Cup anemometers CSAT 3D sonic anemometers LI-7000 CO ₂ /H ₂ O analyzers
5 1.8	U' v' w' T' CO ₂ , U, V, T (horizontal array)	ATI 3D sonic anemometer CATI/2 2D sonic anemometers, LI-7000
62.2,50.1,39.4,28.7 19.6,10.4,3.1,0.9	CO ₂ , H ₂ O Profile	LI-7000 CO ₂ /H ₂ O analyzer
61.9,49.8,39.1,28.4 18.3,10.1,2.8,0.6	Temperature	Aspirated thermocouples

Subcanopy network observations are available for two campaigns in 2003 (Phase 1, DOY 198-238) and 2004/2005 (Phase 2, DOY 250-366 and 01-32). The subcanopy data complement observations that were made around the central 65-meter tower. The observation and acquisition approach was developed at Atmospheric Sciences Research Center, ASRC (*Staubler and Fitzjarrald, 2005*) and includes a PC operating in Linux, an outboard Cyclades multiple serial port (CYCLOM-16YeP/DB25) collecting and merging serial data streams from all instruments in real time, with the data archived into 12-hour ASCII files.

Observations include CO₂, temperature, H₂O and wind field measurements at 1 Hz (Figure 2), this sufficient to cover advection and storage fluxes (non turbulent fluxes). The

system included a LI-7000 Infrared Gas Analyzer (LI-COR inc., Lincoln, Nebraska, USA), a multi-position valve (Vici Valco Instrument Co., Inc.) controlled by a CR23x Micrologger (Campbell Scientific, Inc., Logan, Utah, USA), which also monitored flow rates. The instrument network array (Figure 2 and Table 1) consisted of 6 subcanopy sonic anemometers: a Gill HS (Gill Instruments Ltd., Lymington, UK) 3-component sonic anemometer at 5 m elevation in the center of the grid and 5 SPAS/2Y (Applied Technologies Inc., CO, USA) 2-component anemometers (1 sonic at center and 4 sonic along the periphery), with a resolution of 0.01 m s^{-1} . The horizontal gradients of $\text{CO}_2/\text{H}_2\text{O}$ were measured in the array at 2 m above ground, by sampling sequentially from 4 horizontal points surrounding the main tower location at distances of 70-80m, and from points at 6 levels on the small Draino tower, performing a 3 minute cycle. Air was pumped continuously through 0.9 mm Dekoron tube (Synflex 1300, Saint-Gobain Performance Plastics, Wayne, NJ, USA) tubes from meshed inlets to a manifold in a centralized box.

A baseline air flow of 4 LPM from the inlets to a central manifold was maintained in all lines at all times to ensure relatively “fresh” air was being sampled. The air was pumped for 20 seconds from each inlet, across filters to limit moisture effects. The delay time for sampling was five seconds and the first ten seconds of data were discarded. At the manifold, one line at a time was then sampled using an infrared gas analyzer (LI-7000, Licor, Inc.). The 6-level CO_2 profile on the 5 m tower was determined in a similar, sequential manner, using a LI-7000 gas analyzer sampling pumped air from all 10 points (6 vertical, 4 horizontal) in the measurement array. Flow rates at the inlets were checked regularly to ensure proper flow and to detect potential leaks.

2.3. Preinstallation intercomparison

Following *Staebler and Fitzjarrald* [2004] an initial instrument intercomparison was made to identify the performance of the integrated subcanopy observation system. The CO₂ sensor (Licor 7000 sensor) and the sonic anemometers (CATI/2 and SPAS/2Y, Applied Technologies, Inc. sensors) were co-located on the small tower for a calibration period (5 days) before being deployed at 1.8 meters above the ground (Figure 2). We anticipated that the horizontal transport product uc would be near its largest value at this height, a finding later confirmed at this site (see Figure 4 below). We had insufficient instrumentation to construct a network of towers to measure the CO₂ concentration up to canopy top, and this led us to continue our earlier practice of asserting a profile similarity hypothesis, where one hypothesizes spatial similarity between vertical CO₂ and wind profiles and their product (the horizontal transport). Using a single gas analyzer with a common path multi-position valve for the horizontal and vertical profiles minimizes the potential for systematic concentration errors. A field calibration was performed by co-locating sensors and gas inlets at the same point of measurement. The comparisons indicate scatter in [CO₂] because samples were sequential, not synchronous. The mean standard error was < 0.05 ppm. The wind comparisons were made using a 3D sonic as the standard for the 2D sonic anemometers, resulting in a mean standard error of about 0.005 ms^{-1} . Ambient subcanopy wind speed was on the order of a few cm s^{-1} and can be reliably measured in the subcanopy space by the system. After intercomparison, the sonic anemometers and the CO₂ inlet tubes were moved from the small tower center point and deployed about 2 meters above ground as indicated in Figure 2.

We examined to what extent the subcanopy sensor geometry of CO₂ allows the system to function as a “*network*”, where each point of the measurements are correlated and the space

between them is on the order of the relevant scales of transport or smaller. We test whether the network can be used to capture the relevant gradients and transport processes in very low wind conditions [Staebler and Fitzjarrald, 2004]. Figure 3 (left panel) shows the 3-min data autocorrelation of CO₂ and wind fields determined from continuous measurements.

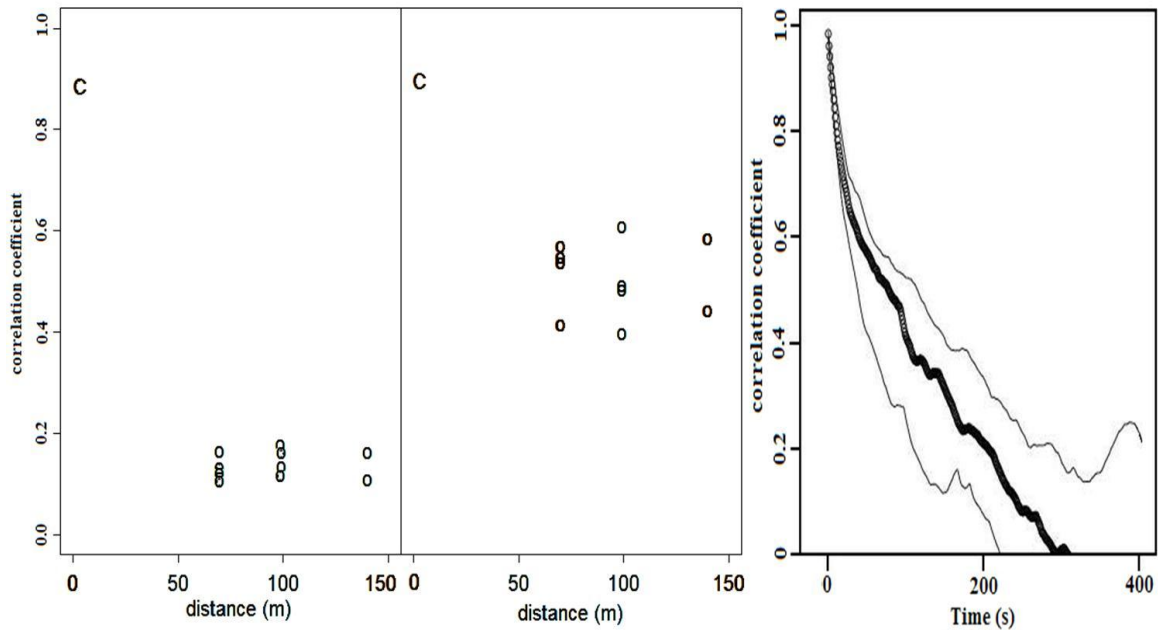


Figure 3. The autocorrelation coefficient for total wind speed (left panel) and CO₂ concentration (center panel) as a function of distance between sampling points 1.8m above ground in the subcanopy. (3-minute averages data from “Draino” Phase 1 (DOY 198-238/2003). “C” represents the calibration period. The right panel shows the temporal autocorrelation for wind, the solid line represents the median, and the thinner lines the upper and lower quartiles. Mean wind speed in the subcanopy was $0.13 \text{ m}\cdot\text{s}^{-1}$.

The relevant spatial scale X is approximately 70-150 m. We assessed our choice of network size by examining observed spatial and temporal autocorrelations of the wind measurements. The spatial autocorrelation of horizontal wind speed (Figure 3 - center panel) drops rapidly to 0.2 in 60 m, but fluctuations in CO₂ (Figure 3 - left panel) exhibit a larger integral scale 100-200 m, while the temporal integral is approximately 100-300s (Figure 3, right panel). This is consistent with results obtained by *Staebler and Fitzjarrald* [2004] in a very different forest, except that the characteristic horizontal CO₂ scale is larger than that at

Harvard Forest, consistent with the thicker canopy at the Tapajós National Forest. We do not understand why the spatial correlations do not decrease with increasing distance, as was observed in *Staedler and Fitzjarrald* [2004]. This could be a consequence of the temporal scale variations being larger than are the spatial ones.

2.4. CO₂ conservation equations

The net ecosystem exchange (NEE) for a horizontal plane at height h , which represents the exchange rate between forest and atmosphere, is given by,

$$NEE_h = F_0 + \int_0^h \bar{s} dz \quad (1),$$

where F_0 is the soil flux entering (or leaving) the control volume at the bottom and the \bar{s} integral describes the sum of all sources and sinks in the canopy space. The Reynolds average conservation equation of a scalar “ c ”, ignoring molecular diffusion process, can be expressed by,

$$\frac{\partial \bar{c}}{\partial t} + \bar{u}_i \frac{\partial \bar{c}}{\partial x_i} + \bar{c} \frac{\partial \bar{u}_i}{\partial x_i} + \frac{\partial \overline{u_i'c'}}{\partial x_i} = \bar{s} \quad (2),$$

with $\bar{u}_i = (u, v, w)$. Considering using equations 1 and 2, and considering incompressibility, after integrating vertically, it can be written in the form,

$$\int_0^h \frac{\partial \bar{c}}{\partial t} dz + \int_0^h \bar{u} \frac{\partial \bar{c}}{\partial x} dz + \int_0^h \bar{v} \frac{\partial \bar{c}}{\partial y} dz + \int_0^h \bar{w} \frac{\partial \bar{c}}{\partial z} dz + \int_0^h \frac{\partial \overline{u'c'}}{\partial z} dz + \int_0^h \frac{\partial \overline{v'c'}}{\partial z} dz + \left(\overline{w'c'} \right)_h = \int_0^h \bar{s} dz \quad (3),$$

$$[1] \quad [2] \quad [3] \quad [4] \quad [5] \quad [6] \quad [7] \quad [8]$$

where u , v , and w , are wind components and “ c ” a scalar, such as CO₂. The term [4] is the vertical advection term and term [8] the sum of all sinks and sources between $z=0$ and $z=h$, including everything crossing the lower boundary at $z=0$.

In the case of horizontal homogeneity, terms [1], storage in the canopy space, and [7], vertical eddy flux at $z=h$ (57.8 m for the site studied), are obtained from standard EC and profile sensors at the flux site. Terms [5] and [6] are the horizontal turbulent flux divergence and negligible when compared with other terms [Yi *et al.*, 2000; Turnipseed *et al.*, 2003]. The terms [2], [3] and [4] respectively are horizontal and vertical advection. The vertical mean advection was integrated using the method of Lee [1998]:

$$[\overline{w\bar{c}}]_0^h - \frac{\overline{w}_h}{h} \int_0^h \bar{c}(z) dz = \overline{w}_h \left(\bar{c}(h) - \frac{1}{h} \int_0^h \bar{c}(z) dz \right) \quad (4),$$

where \overline{w}_h and $\bar{c}(h)$ are the residual vertical velocity and the mean concentration at the top of the layer (57 m), respectively [see in Staebler and Fitzjarrald, 2004]. Staebler and Fitzjarrald [2004] argued that Lee's approach is an overestimate, noting that the assumption of a linear increase of \overline{w}_h with height is often violated. Comparisons of the divergence measurements at 1.8 m height with measured vertical velocities at 46 m and 57.8 m were made for a few days of wind data and the results show no correlation indicating that Lee's approach is also violated for the site studied here. However, Lee's formulation will be used to provide an upper estimate of the vertical advection term in order to compare its potential significance relative to the other terms. The calculation of mean vertical advection was made only during phase 2 (DOY 250-366/2004 and 01-32/2005) when sufficient data for the calculation was available. We recognize that obtaining credible mean vertical velocity from sonic anemometers is still a challenge (e.g., Vickers and Mahrt, [2006]). However, the difficulties in assessing one term in the continuity equation should not preclude efforts to obtain the others.

2.5. Vertical integration of the horizontal advection terms

To perform a complete three-dimensional forest CO₂ box budget it is necessary to obtain vertical profiles of the horizontal gradient measurements for the entire control volume, and this is generally not feasible. We lacked resources to install a network of towers to measure the CO₂ profile at a number of locations in the canopy. Noting, as in *Staebler and Fitzjarrald* [2004], that the product uc is largest near the forest floor, we relied on subcanopy measurements made 1.8 m above the ground. To compensate for the missing network of vertical profiles, we approximate the vertical integration through the canopy of the horizontal advective terms [2] and [3] following methods developed by *Staebler and Fitzjarrald* [2004]. One hypothesizes spatial similarity between vertical CO₂ and wind profiles and their product (horizontal transport) uc , where \underline{u} is the average wind and \underline{c} the average CO₂ concentration. In this assumption, the shapes of the profiles throughout the canopy space are considered similar to the central point where the profiles are measured (Figure 2).

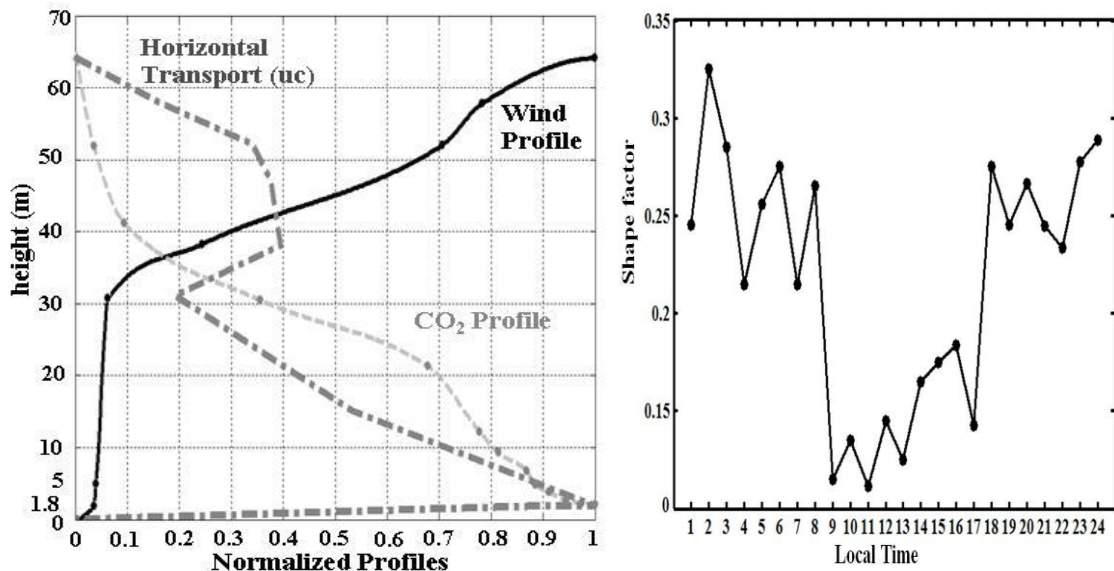


Figure 4. Typical nighttime normalized median profiles of CO₂, wind speed and their product (uc) horizontal transport (left panel); and the diurnal cycle of the shape factor for horizontal advection (right panel).

Figure 4 presents a typical feature of the shape factor profiles of CO₂ concentration, wind and horizontal transport. The horizontal subcanopy measurement height (1.8 m) is a height where the advection term is expected to be significant, providing confidence for single level height measurements to determine the integrated layer advection.

The procedure of integrating vertically is formalized through,

$$c^*(x, z) = f(z) c^*(x, z_1) \quad , \quad (5)$$

where $f(z)$ is the (assumed constant) shape of the CO₂ profile relative to height $z_1 = 1.8\text{m}$ (horizontal plane). The difference between the actual CO₂ concentration and nocturnal CO₂ concentration above the canopy (baseline value) is defined as $c^*(z) = c(z) - c_0$. The c^* was used instead of c because there is a practical lowest limit of CO₂ = c_0 , indicative of the atmospheric base state, since it has no effect on the budget. Then, the vertical integration gives:

$$\int_0^h \frac{\partial c^*(x, z)}{\partial x} dz = \frac{\partial c^*(x, z_1)}{\partial x} \int_0^h f(z) dz = \frac{\partial c^*(x, z_1)}{\partial x} h S_c \quad (6),$$

where S_c is the shape factor for the CO₂ concentration profile. Applying the same procedure to describe the wind speed profile yields the advection estimates:

$$\begin{aligned} \int_0^h u(x, z) \frac{\partial c^*(x, z)}{\partial x} dz &= \int_0^h g(z) u(x, z_1) f(z) \frac{\partial c^*(x, z_1)}{\partial x} dz = \left(u(x, z_1) \frac{\partial c^*(x, z_1)}{\partial x} \right) \int_0^h f(z) g(z) dz \\ &= \left(u(x, z_1) \frac{\partial c^*(x, z_1)}{\partial x} \right) \cdot (hS) \end{aligned} \quad (7),$$

where S is the shape factor for horizontal advection of CO₂. The nocturnal time shape factor values for both studied periods averaged 0.28, while the daytime value was typically 0.14 (Figure 4). This is consistent with results obtained by *Staebler and Fitzjarrald* [2004], possibly due to similar shape factors for CO₂ and wind speed profiles at both sites.

3 – Results and Discussion

3.1. CO₂ concentration field

The average composite of horizontal concentration of CO₂ measured at 2-m height in nocturnal conditions for Phase 1 and Phase 2 (Figure 5) shows that the horizontal CO₂ field varied significantly at night during both observation phases. During Phase 1, the CO₂ concentrations at night were higher than during Phase 2. This may be associated with vegetation response to drier, cooler conditions and lighter wind during this phase, according to Figure 6.

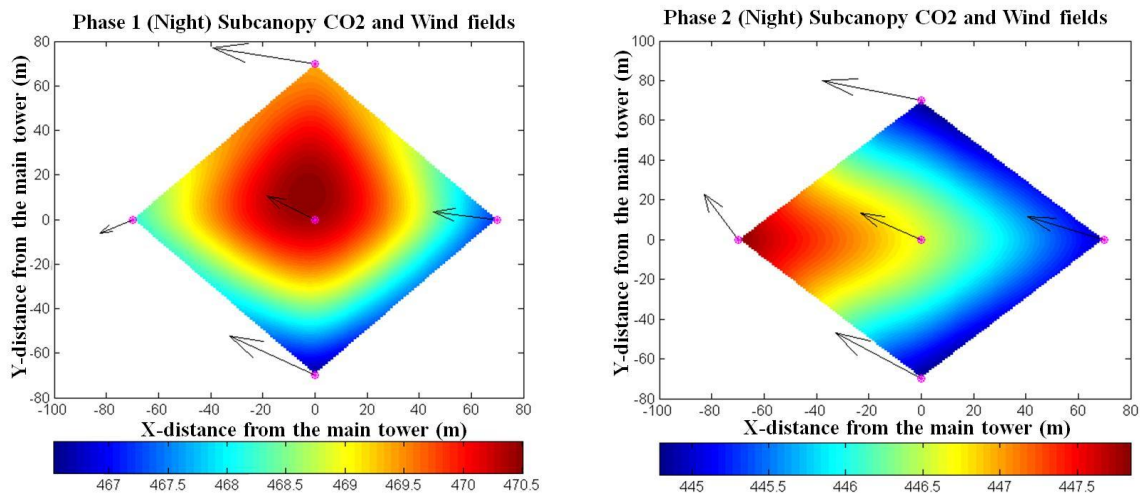


Figure 5. Night time composite of averaged subcanopy CO₂ concentration field and wind vectors for Phase 1 and Phase 2 campaigns. The units are in ppm and ms⁻¹, respectively. (Largest arrow is 0.15 m s⁻¹)

The typical values of average horizontal CO₂ gradients were about $-0.026 \left(\frac{\partial \bar{c}}{\partial x} \right)$, East-West) and $0.023 \left(\frac{\partial \bar{c}}{\partial y} \right)$, North-South) ppm m⁻¹ for all nights considered (7390 and 18366 average 3-minute data values, Phase 1 and Phase 2, respectively). These results are

comparable to the range of horizontal CO₂ gradients that have been reported in the literature, 0.025 to 0.079 ppm m⁻¹ [Feigenwinter et al., 2004; Staebler and Fitzjarrald, 2004; Aubinet et al., 2005]. One expects CO₂ concentrations and gradients near the ground to be site-specific under calm night wind speed conditions, due to varying soil respiration rates that depend on soil and litter layer composition, temperature and moisture.

Vertical profiles of temperature, water vapor concentration, CO₂ concentration and wind speed characterize the microclimate observed during each phase (Figure 6). The drier Phase 1 presents daytime and night patterns that contrast with the wetter Phase 2 conditions.

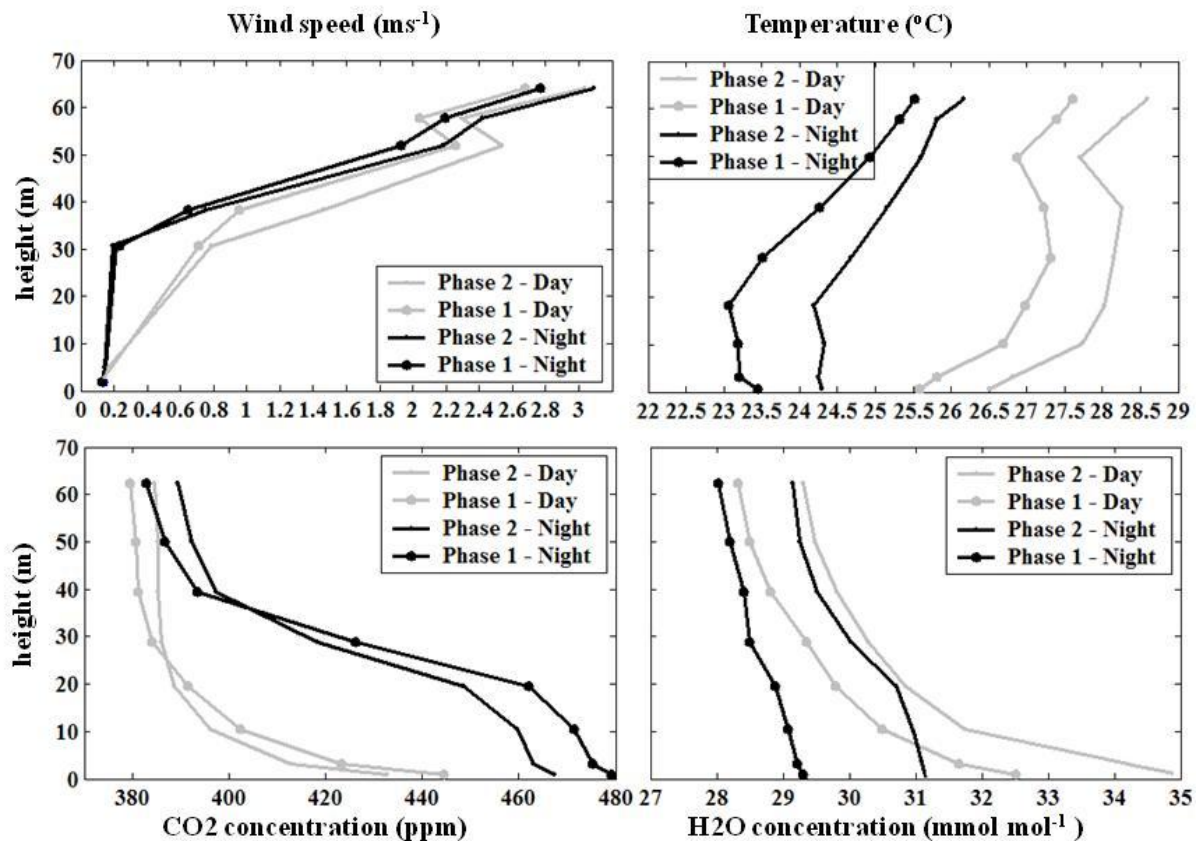


Figure 6. Vertical profiles of concentration of CO₂, wind speed, temperature, and water vapor, for both Phases (dry and wet).

The wind speed profile had a similar shape during both phases, but above the canopy the magnitude of wind speed was greater in Phase 2 compared with Phase 1 period. This

suggests a reduction on turbulence level or vertical mixing during the nighttime, as shown in Figure 7. The temperature profiles show the same pattern for the two phases, however, the dry phase was about 2°C warmer. During the daytime, for both dry and wet periods, a maximum air temperature was observed at 30 m associate with the absorption of sunlight by vegetation, generating a light unstable condition between 30 and 50 m, and stable condition below 30 m.

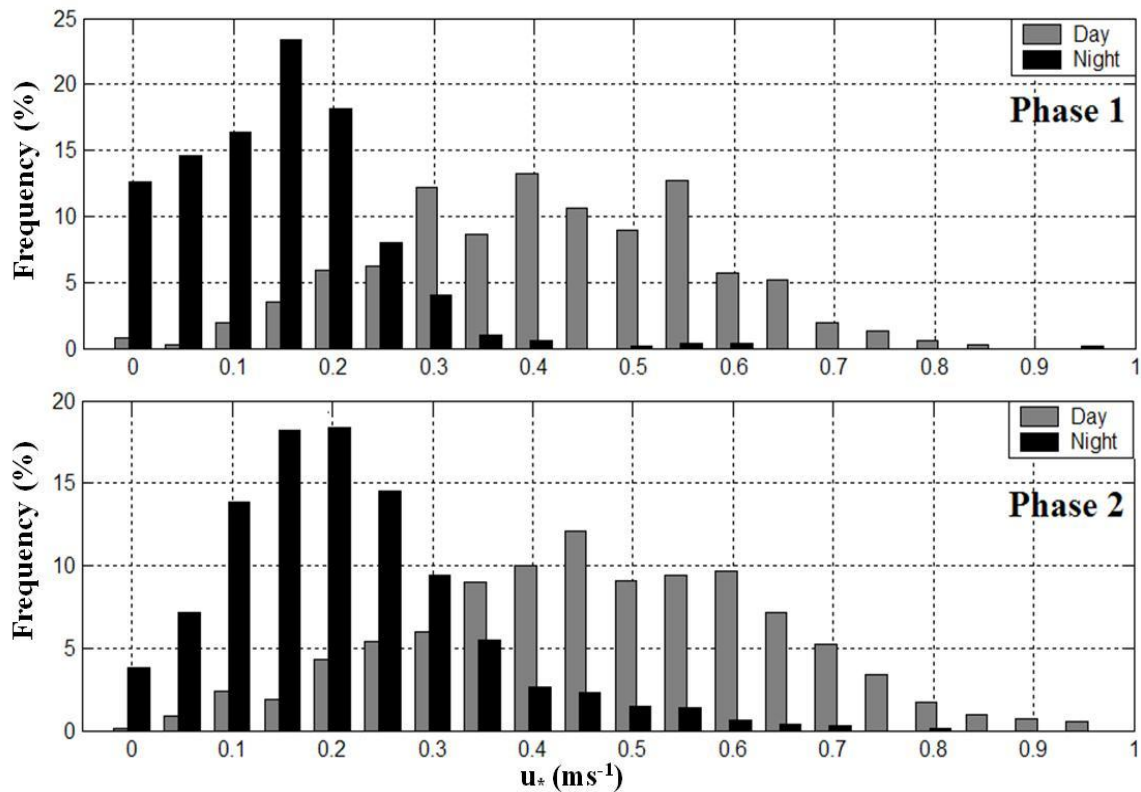


Figure 7. Frequency distribution histogram of friction velocity (u_*) at 57.8 m, for Phase 1 and Phase 2 measurements, separate day and night periods.

During the nighttime the net loss of thermal radiation cooled the vegetation relative to the air adjacent, generating local stability and affecting above-canopy momentum transport. However, from the observed temperature profiles, in the layer below 20 m, trunk space layer, just below the upper canopy; the subcanopy temperature profile was dry and cold relative to the underlying air ($\approx -0.25^\circ\text{C m}^{-1}$). This combination of the cooling above 20 m and warming

below generates instability associated with negative buoyancy [see also *Fitzjarrald et al.*, 1990; *Fitzjarrald and Moore*, 1990]. This process may be contributing or creating horizontal flow gravitationally such as suggested by *Lee* [1998]. Similar temperature profiles were reported by *Goulden et al.*, [2006] for km83 LBA site 16 km away to the south.

As expected, the vertical concentration of CO₂ reflects both atmospheric transport and forest physiological processes, in which during the daytime photosynthesis removes CO₂ from the air depleting concentration levels, and during the nighttime the concentration builds up due to respiration, the reduction of turbulence, and absence of photosynthesis.

The frequency distribution of the friction velocity above the canopy for the both dry (Phase 1) and wet (Phase 2) periods (Figure 7) shows very small values at nighttime. Nocturnal values of friction velocity smaller than 0.2 ms⁻¹ accounted for more than 85% and 65% for dry and wet periods, respectively. Therefore, we define deficit nights, using the procedure outlined by *Staebler and Fitzjarrald* [2004], when NEE (CO₂ eddy flux plus storage term) was less than total ecosystem respiration (see *Saleska et al.* [2003] and *Hutyra et al.* [2007], for details of these datasets). About 130 selected nights in each period, Phase 1 and Phase 2 match these criteria and were considered calm nighttime conditions.

Recently, *Saleska et al.* [2003] and *Miller et al.* [2004] have used a cutoff value of 0.3 ms⁻¹ for u_* correction to NEE estimates for the site studied. As show in Figure 7, much of the observed data must be discarded using this criterion, possibly altering the results. As reported by *Miller et al.* [2004], the tropical forest in Amazonia becomes a source than sink of atmospheric CO₂ depending of the cutoff value u_* used.

3.2. Subcanopy horizontal wind field

To calculate horizontal advection (terms [3] and [4] Equation 3), we estimated the horizontal wind field on the subcanopy space using the measurement subcanopy network described above. Though the site was considered flat in earlier reports [*Saleska et al.*, 2003; *Miller et al.*, 2004], a high resolution image shows that the forest floor gently slopes in a west-northwest direction from the main tower, according to Figure 2. *Goulden et al.* [2006] inferred the presence of drainage flows toward the SE at the km83 site to the south of the present study site, but they did not demonstrate subcanopy motion forced by density anomalies. Figure 8 shows statistics of the subcanopy wind field at night. There is a persistent wind direction that follows the local topographic gradient (see also Figure 1).

These nocturnal horizontal wind directions are in accord with nocturnal wind directions observed at the Jamaraguá station (Figure 1) close to the river Tapajós [*Fitzjarrald et al.*, 2004]. The statistics indicate that the nocturnal horizontal wind magnitude, varies among the subcanopy measurement points, probably due to the large heterogeneity of vegetation structure obstructions [see also *Staebler and Fitzjarrald*, 2004]. The average magnitude of the horizontal wind field in the subcanopy varied from 0.1 to 0.45 m s⁻¹.

The observed subcanopy wind direction was prevailing from the southeast, with an interesting shift compared to the top of the main tower (57.8 m) wind direction, indicating a clearly uncoupled situation (Figure 8). Apparently, it seems that the subcanopy flow responds primarily to the local terrain gradients. *Goulden et al.* [2006] have reported a similar shift of the wind direction following the terrain gradient, even at 20 m when compared against the 64 m wind direction (see Figure 6, pg. 8 there in). *Sun et al.*, [2007] have also indicated that this shift happen at large spatial scales using short term datasets.

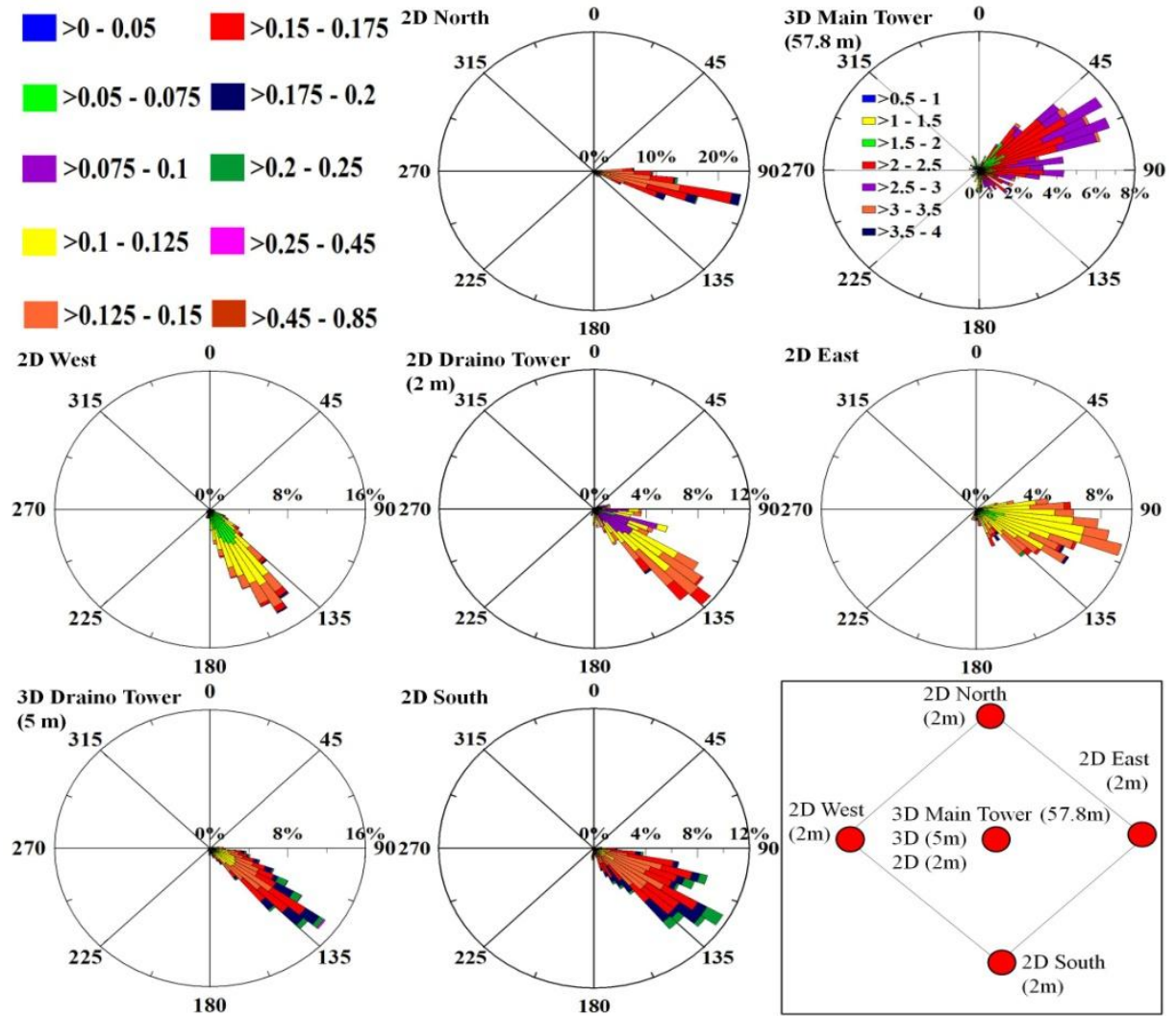


Figure 8. Nighttime distribution of the wind rose and its magnitude (m s^{-1}) for the Draino sonic anemometer network and at top of main tower (57.8 m), including its localization (see Figure 2).

3.3. Subcanopy flow forcing terms

We follow the analysis presented by *Staebler and Fitzjarrald* [2004]. Subcanopy flows are generated by the balance of three driving forces; the pressure gradient perturbations, the buoyancy and the stress divergence, according to the momentum equation. The

momentum equation is given by, $\frac{\partial u}{\partial t} + u \frac{\partial u}{\partial x} + w \frac{\partial u}{\partial z} = -\frac{1}{\rho} \frac{\partial p'}{\partial x} - g \frac{\theta'_v}{\theta_v} \frac{\partial h}{\partial x} - \frac{\partial \tau}{\partial z}$, where ρ is the

density, p' the pressure perturbation, θ_v the virtual temperature, θ_v' the local departure of θ_v from the mean, $\frac{\partial h}{\partial x}$ the topographic slope, and τ is the vertical stress, and drag effects are ignored. We do not believe that the terrain at the site studied is not so steep as to produce pressure perturbations strong enough to affect subcanopy flow locally, and it is ignored in the subsequent analysis. Thereby, the relative importance of buoyancy ($b_{term} = \left| g \frac{\theta_v'}{\theta_v} \frac{\partial h}{\partial x} \right|$) and stress divergence ($t_{term} = \left| \frac{\partial \tau}{\partial z} \right|$) terms will be considered. Observed fractions of the buoyancy term ($b_{term}/(b_{term}+t_{term})$) and stress divergence term ($t_{term}/(t_{term}+b_{term})$) indicate that the buoyancy term was more important during the nighttime than was the stress divergence term (Figure 9). The stress divergence term was more significant during the daytime associated with a higher degree of turbulent mixing as expected (Figure 9).

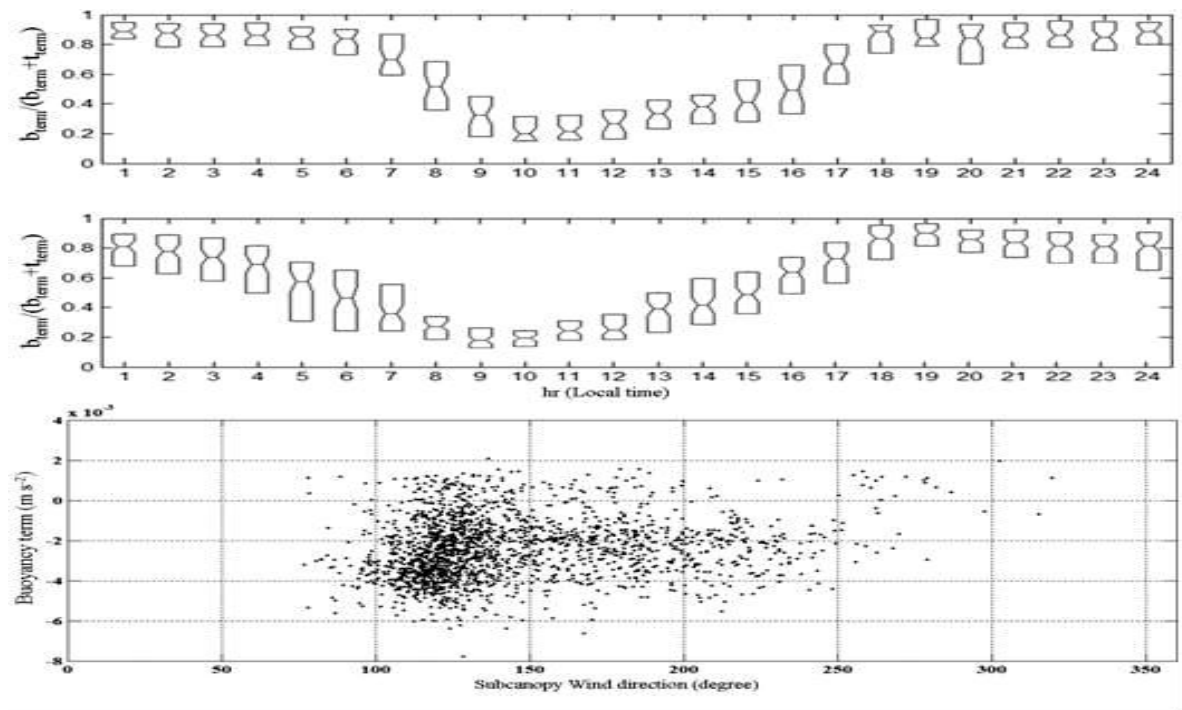


Figure 9. Diurnal cycle of buoyancy term forcing fractions relative to stress divergence term for Phase 1 (top panel) and Phase 2 (middle panel) observations, and (bottom panel) the buoyancy forcing term vs. subcanopy wind direction for both Phases.

Flows generated by the buoyancy term force the flow down the dominant terrain slope. Nocturnal wind directions were predominantly from the southeast toward northwest, as would be expected given the local topographic gradient (Figure 1). Our observations strongly indicate that the negative buoyancy term is the physical mechanism that explains the nocturnal drainage flow at this relatively flat study site.

3.4. Estimates of Advection Terms

The horizontal advection terms ([2] and [3] in Equation 3) were estimated using subcanopy wind speed components and CO₂ observation datasets from Phase 1 and Phase 2 (14350 and 36459 3-min valid observations, respectively). The horizontal CO₂ gradients were calculated using a linear least-square planar fit (Figure 5). (Note that the interpolated fields shown in Figure 5 were not used in the calculation).

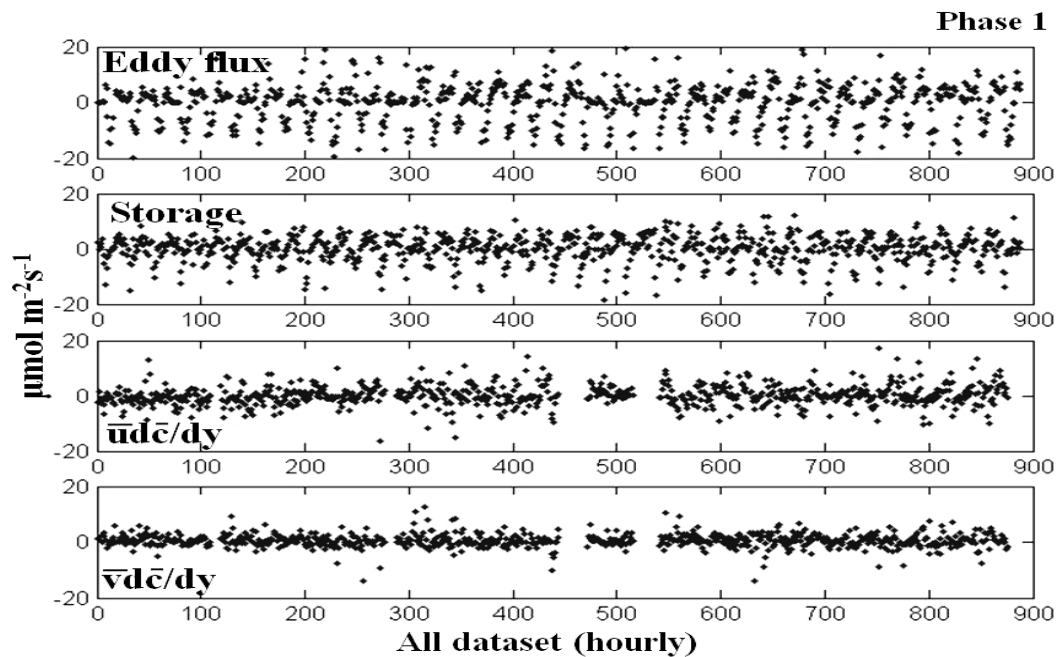


Figure 10a. Hourly-averaged summary of results for the Phase 1 and all the terms except eddy flux are average values for 0 to 57.8 m control volume. Top panel: vertical eddy flux at 57.8 m; 2nd panel: storage; 3th panel: east-west advection; and 4th panel: south-north advection, terms.

The hourly time series of average measurement flux terms for the CO₂ budget (Figure 10a and 10b) illustrate that the advective terms and eddy flux are of comparable magnitude, in accordance with recent published results at other sites [Staebler and Fitzjarrald, 2004; Aubinet et al., 2005; Marcolla et al., 2005; Sun et al., 2007; Feigenwinter et al., 2008]. Although the advective terms exhibit large scatter, their magnitude is comparable to the other flux terms. When averaged over all periods (for wet and dry phases) we obtained values significantly different from zero. For both phases (dry and wet) at the site studied, indicate a positive contribution to the total flux (i.e. transporting CO₂ out of the control volume around the tower).

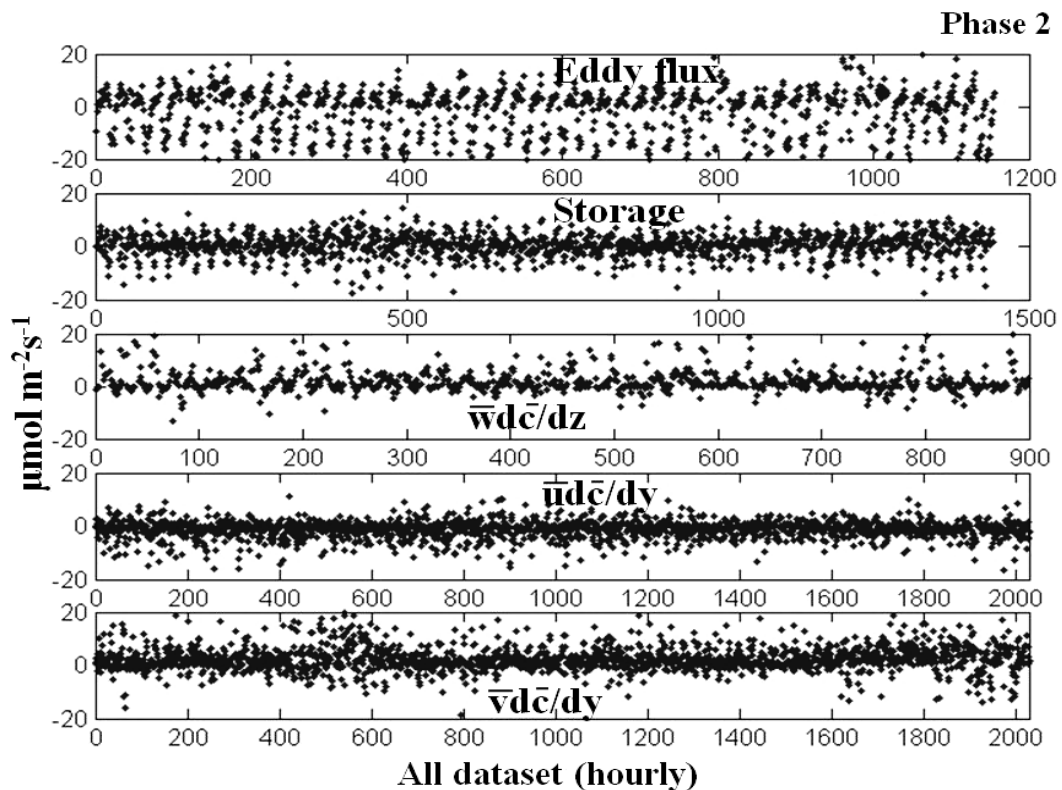


Figure 10b. Hourly-averaged summary of results for the Phase 2 and all the terms except eddy flux are average values for 0 to 57.8 m control volume. Top panel: vertical eddy flux at 57.8 m; 2nd panel: storage; 3rd panel: vertical advection; 4th panel: east-west advection; and 5th panel: and south-north advection, terms.

The average diurnal cycle of the flux terms for both dry (Phase 1) and wet (Phase 2) periods (Figure 11a and 11b) show the expected diurnal eddy flux pattern, negative during the day and positive at night. The vertical advection term plays no important contribution on average, but has a positive sign, since the mean vertical velocity and vertical CO₂ gradients were negative. The observed storage term is positive during the night, corresponding to CO₂ build-up in the canopy during stable conditions, and negative in the morning, owing to the release of the accumulated CO₂ due to mixing and onset of photosynthesis.

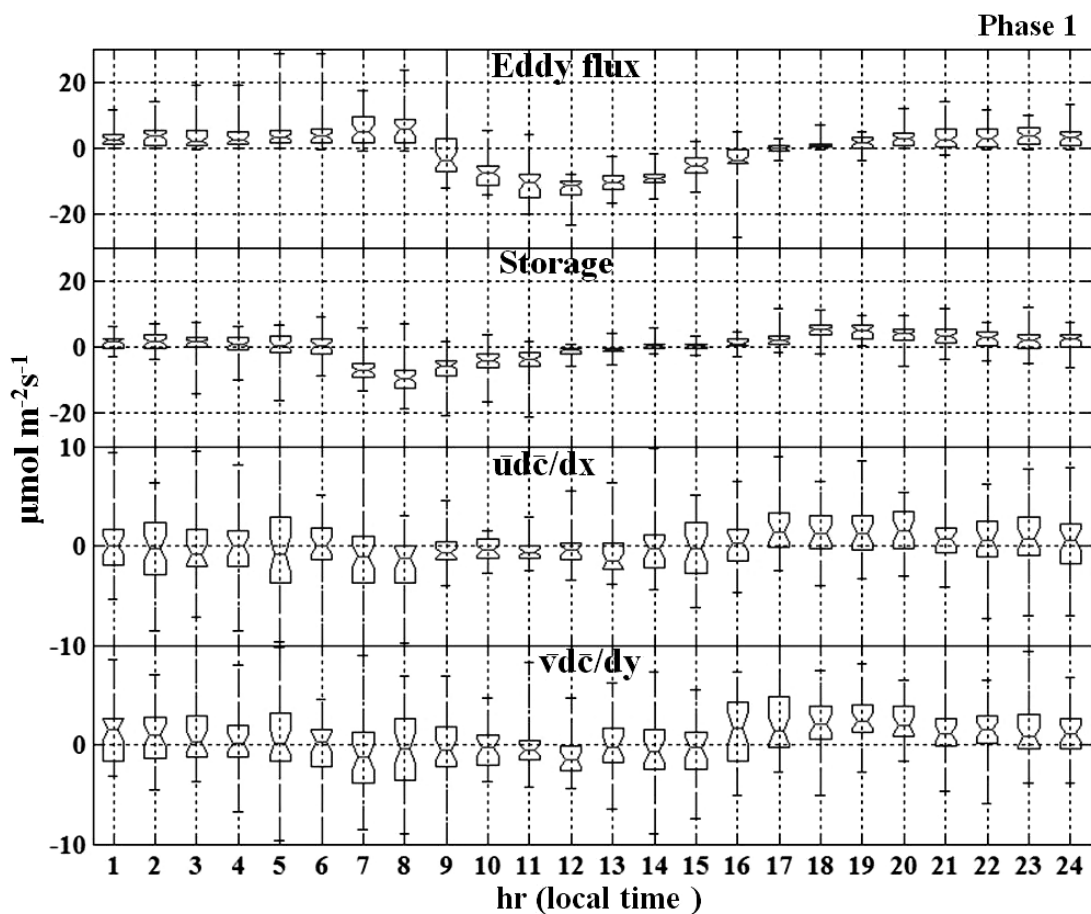


Figure 11a. Top panel: Hourly-averaged vertical eddy flux at 57.8 m; 2nd panel: storage term; 3rd panel: east-west advection term; and 4th panel: and south-north advection, terms. Note the change in vertical scale between the phases.

A notable feature in Figure 11a and 11b is that CO₂ storage during the second part of the night (between 01 - 06 LT) was 2 to 3 times smaller than the CO₂ storage in first part

(between 17 - 22 LT). This variability might be explained partially by differing CO₂ respiration source intensity from soil, canopy air space stability and canopy structure, but also could have resulted from the drainage flows. Similar patterns were observed by *Yang et al.*, [1999] in a Boreal Aspen Forest (USA), see Figure 3 there in. *Aubinet et al.* [2005] made this hypothesis, but did not demonstrate it observationally. It appears that between 1 and 6 LT our observations are consistent with significant positive horizontal advection, transport out of the control volume. The 17-22 LT observations also show positive horizontal advection. However, the high ecosystem respiration rate maintains a large storage term, and this partially offsets this horizontal advection in the CO₂ budget.

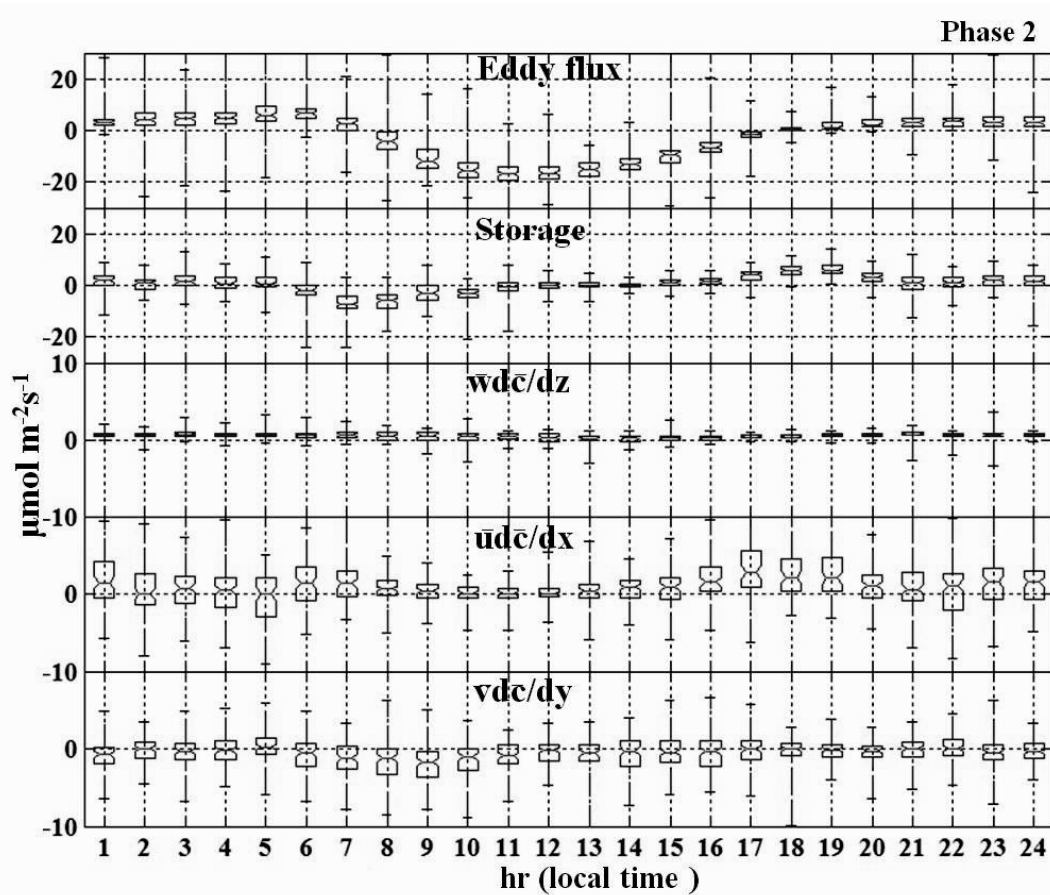


Figure 11b. Top panel: Hourly-averaged vertical eddy flux at 57.8 m; 2nd panel: storage term; 3rd panel: vertical advection term; 4th panel: east-west advection term; and 5th panel: and south-north advection terms. Note the change in vertical scale between the phases.

3.5. CO₂ budget

To determine the relative contribution of the nocturnal advection terms to the CO₂ budget, we compare the mean nocturnal variation of NEE (eddy flux + storage) with and without considering the observed advection terms and ecosystem respiration during dry (Phase 1) and wet (Phase 2) periods of observation (Figure 12a and 12b).

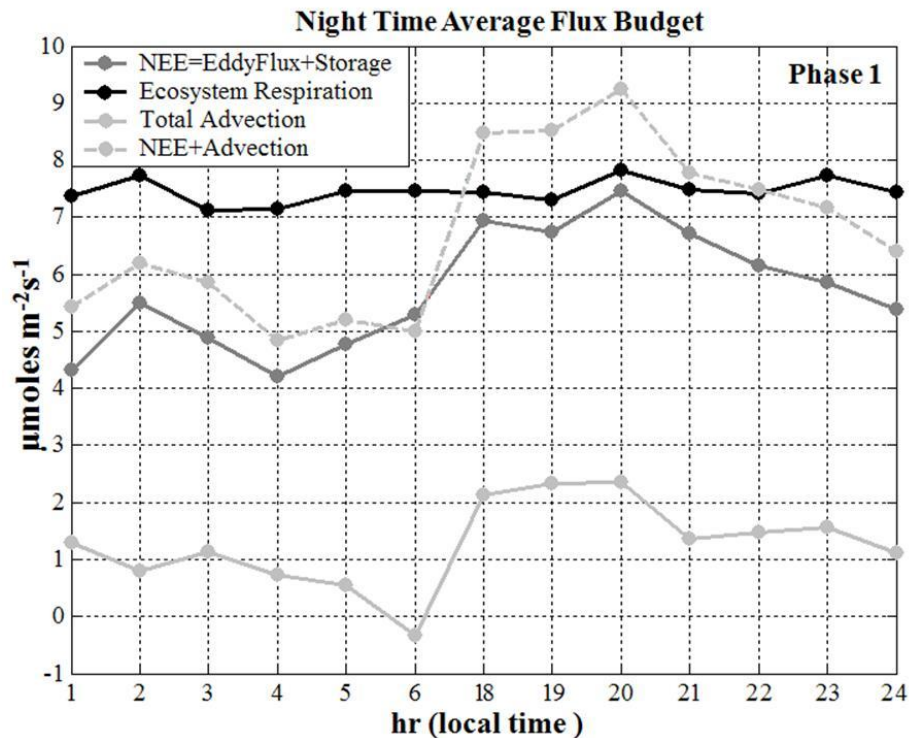


Figure 12a. Mean nocturnal variation of the NEE (Eddy covariance flux + storage), ecosystem respiration, horizontal advection and NEE plus advection, for Phase 1 (Dry period).

The ecosystem respiration, EC flux, and storage were measured by the CD-10 group [Saleska *et al.*, 2003; Hutryra *et al.*, 2007]. Results show that the differences between NEE and ecosystem respiration are improved when the advection term is accounted for (Table 2 and Figure 12a and 12b). The advection term accounts for $1.27 \mu\text{mol m}^{-2}\text{s}^{-1}$ and $0.91 \mu\text{mol m}^{-2}\text{s}^{-1}$, for Phase 1 and Phase 2 respectively, representing 71% and 73% of the observational ‘deficit’ between ecosystem respiration and NEE.

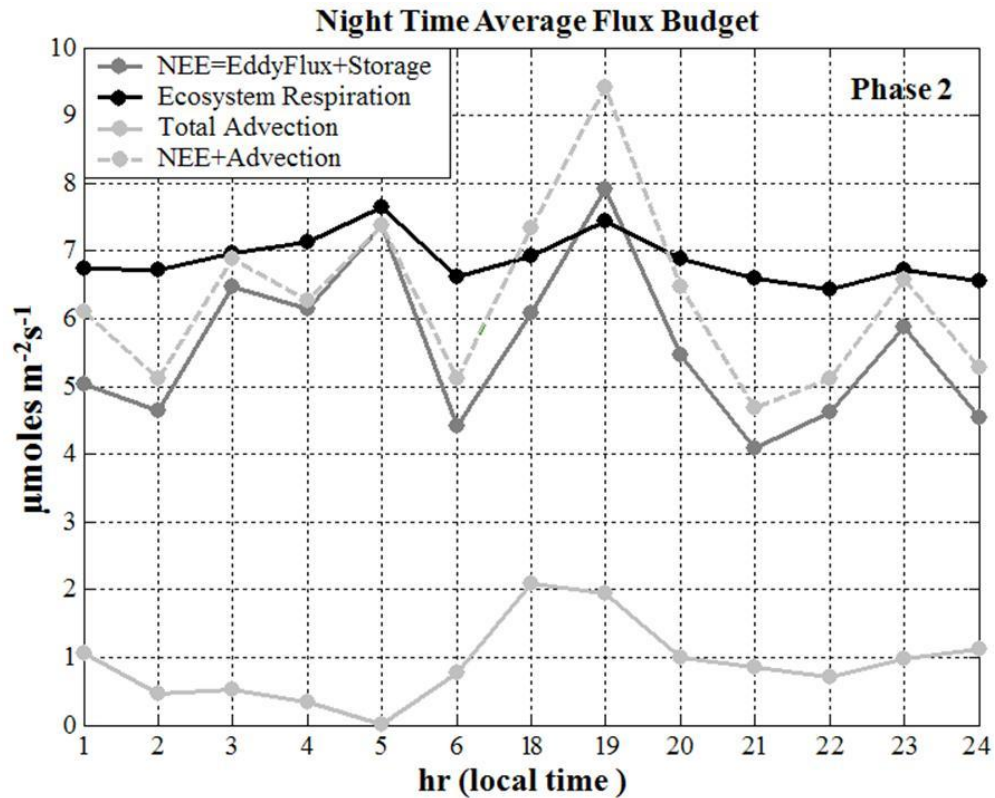


Figure 12b. Same Figure 12a, for Phase 2 (Wet period).

Table 2. Summary of mean nocturnal CO₂ budget for Phase 1 and Phase 2

Flux components ($\mu\text{mol m}^{-2} \text{s}^{-1}$)	Phase 1	Phase 2
NEE	5.71	5.58
Respiration	7.45	6.87
Deficit	1.74	1.29
Advection	1.27	0.91
NEE + Advection	6.98	6.49

3.6. Correlation between advection components and friction velocity

For the site studied here, the threshold value for friction velocity [e.g., *Falge et al.*, 2001; *Gu et al.*, 2005] was reported by *Saleska et al.* [2003] and *Miller et al.* [2004] to be between 0.2 and 0.3 m s⁻¹. Is the assumption that advection is only significant below this

threshold valid? Our results show a clear dependence of the advection term on friction velocity for both observation periods (Figure 13). There is a significant positive advection contribution to the CO₂ budget that should be included in the NEE calculation, even when the friction velocity is higher than the threshold values commonly used. Our results in the Tapajós forest indicate that this interval lies between 0.3 and 0.6 m s⁻¹.

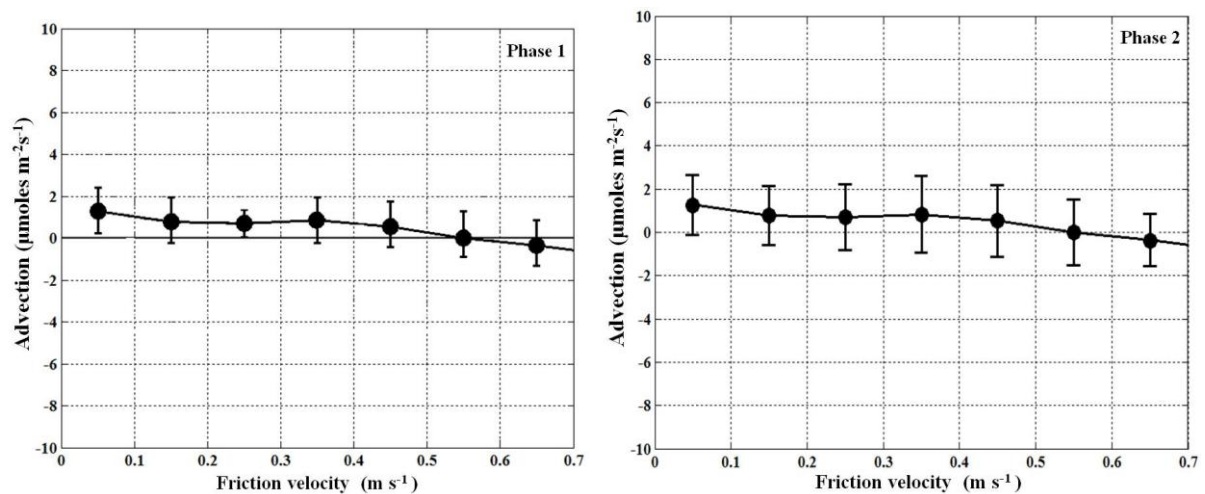


Figure 13. Mean nocturnal variation of the advection term as a function of the friction velocity rank, for Phase 1 (left panel) and Phase 2 (right panel) datasets. Solid line with dots indicates binned average values (0.1 intervals). Error-bar also is plot with standard deviation, respectively.

4. Summary and Conclusions

We present results of the first effort to determine observationally the importance of the nocturnal advection processes on the CO₂ budget in the Amazon tropical rain forest. We tested the hypothesis that persistent nocturnal subcanopy horizontal advection exists and transports an important amount of CO₂ out of the control volume at one old-growth tropical

rain forest site. We determined the magnitude of the horizontal subcanopy gradients of CO₂ and of the wind field and found sufficient net horizontal advection to affect the CO₂ budget.

The methodology established by *Staebler and Fitzjarrald* [2004, 2005] was applied and tested to measure the subcanopy scalar gradients and wind field. These data were complemented by eddy flux and mean profile observations made at the same site on a 65-m tower (section 2). The measurements were performed in the dry season (DOY 198-238 2003 - Phase 1) and in the wet season (DOY 278-366 2004 and 1-32 2005 - Phase 2). The horizontal gradient of the CO₂ concentration and average wind speed, were on the order of 0.02 ppm m⁻¹ and 0.12 m s⁻¹, respectively (section 3.1).

Prevailing subcanopy wind directions were from the southeast and were well correlated with gentle undulations of the landscape near the tower. The tropical forest subcanopy near the forest floor was stable at all times of day, but it was more pronounced during all 130 selected nights analyzed (section 3.2). That there was little coupling with the flow aloft indicates that there is potential for lateral export of subcanopy CO₂ even during the daytime, when this effect is often ignored. The negative buoyancy term was the principal physical mechanism responsible for generating the nocturnal subcanopy flow. During the daytime the stress divergence term was dominant, suppressing the dominance of the buoyancy effect (Section 3.3).

The results from direct measurements of the horizontal gradients of CO₂ and wind speed components measured in the subcanopy indicated that their magnitudes were sufficiently significant to produce a net nocturnal horizontal advection average between 0.91 and 1.27 μmol m⁻² s⁻¹ for dry and wet observation periods, respectively. Nocturnal horizontal advection was of the same order as the vertical EC and storage flux components. Depletion of the storage component was due in large part to net positive horizontal advection, primarily during the second part of the night (01 – 06 LT; section 3.4).

Comparison of the nocturnal deficit from ecosystem respiration and NEE measured on the eddy flux tower demonstrated the important contribution of the mean nocturnal horizontal advection on the atmospheric CO₂ budget. The mean nocturnal advection component represented 73% and 71% of this deficit for dry and wet periods analyzed (130 nights), respectively.

This suggests an important role of the nocturnal advection for the total CO₂ budget at this site. It was also verified that for nighttime intervals, with friction velocity between 0.3 and 0.6 m s⁻¹ (commonly accepted as sufficient to provide correct nighttime eddy fluxes), there was a positive net horizontal transport of CO₂ by the advection component. Therefore, even under considerable high turbulence levels at night, horizontal advection transport in the total CO₂ budget is significant.

These results confirm that few sites are flat enough that horizontal advective effects can be ignored *a priori*. In future work the validity of the CO₂ profile similarity hypothesis we invoked to introduce *shape factors* in (4) should be linked explicitly to the observed mean vegetation profile. Observational estimates of the effect of mean vertical velocity on scalar budgets may be the major source of uncertainty in the budget. Continuous, long-term observations with redundant instrumentation are needed to clarify this issue.